Author Manuscript Published OnlineFirst on November 19, 2019; DOI: 10.1158/1541-7786.MCR-19-0619
Author manuscripts have been peer reviewed and accepted for publication but have not yet been edited.

Ceramide analog SACLAC modulates sphingolipid levels and Mcl-1 splicing to induce apoptosis in acute myeloid leukemia

Jennifer M. Pearson[1], Su-Fern Tan[2], Arati Sharma[3,6], Charyguly Annageldiyev[3], Todd E. Fox[4], Jose Luis Abad[5], Gemma Fabrias[5], Dhimant Desai[6], Shantu Amin[6], Hong-Gang Wang[3,7], Myles C. Cabot[8], David F. Claxton[3], Mark Kester[4,9], David J. Feith[2,9] and Thomas P. Loughran, Jr[2,9]*

[1] Department of Biochemistry and Molecular Genetics, University of Virginia, Charlottesville, VA, USA
[2] Department of Medicine, Division of Hematology & Oncology, University of Virginia, Charlottesville, VA, USA
[3] Penn State Cancer Institute, Hershey, PA, USA
[4] Department of Pharmacology, University of Virginia, Charlottesville, VA, USA
[5] Department of Biological Chemistry, Networking Biomedical Research Centre on Liver and Digestive Diseases (CIBER-EHD), Institute for Advanced Chemistry of Catalonia, Spanish National Research Council (IQAC-CSIC), Barcelona, Spain
[6] Department of Pharmacology, Penn State College of Medicine, Hershey, PA, USA
[7] Department of Pediatrics, Penn State College of Medicine, Hershey, PA, USA
[8] Department of Biochemistry and Molecular Biology, East Carolina Diabetes and Obesity Institute, Brody School of Medicine, East Carolina University, Greenville, NC, USA
[9] University of Virginia Cancer Center, Charlottesville, VA, USA

*Corresponding Author:
Thomas P. Loughran, Jr.
University of Virginia Cancer Center
P.O. Box 800334
Charlottesville, VA 22908-0334
TL7CS@virginia.edu
(434) 243-9926

RUNNING TITLE

SACLAC induces apoptosis in acute myeloid leukemia

KEYWORDS

acid ceramidase, sphingosine 1-phosphate, splicing factor 3b subunit 1, mRNA splicing, Mcl-1S, AML xenograft

CONFLICT OF INTEREST STATEMENT

Several patents have been issued and licensed from Penn State Research Foundation to Keystone Nano Inc. (Pennsylvania) for proprietary nanoscale formulations that encapsulate therapeutic bioactive lipids, such as the ceramide nanoliposome. Mark Kester is the Chief Medical Officer and cofounder of Keystone Nano, Inc. Thomas P. Loughran, Jr. is on the Scientific Advisory Board and has stock options for both

Keystone Nano and Bioniz Therapeutics. These potential conflicts did not impact the work presented in this manuscript.

ABSTRACT

Acute myeloid leukemia (AML) is a disease characterized by uncontrolled proliferation of immature myeloid cells in the blood and bone marrow. The five-year survival rate is approximately 25%, and recent therapeutic developments have yielded little survival benefit. Therefore, there is an urgent need to identify novel therapeutic targets. We previously demonstrated that acid ceramidase (ASAH1, referred to as AC) is upregulated in AML and high AC activity correlates with poor patient survival. Here, we characterized a novel AC inhibitor, SACLAC, that significantly reduced the viability of AML cells with an EC_{50} of approximately 3 μM across 30 human AML cell lines. Treatment of AML cell lines with SACLAC effectively blocked AC activity and induced a decrease in sphingosine 1-phosphate and a 2.5-fold increase in total ceramide levels. Mechanistically, we showed that SACLAC treatment led to reduced levels of splicing factor SF3B1 and alternative Mcl-1 mRNA splicing in multiple human AML cell lines. This increased pro-apoptotic Mcl-1S levels and contributed to SACLAC-induced apoptosis in AML cells. The apoptotic effects of SACLAC were attenuated by SF3B1 or Mcl-1 overexpression and by selective knockdown of Mcl-1S. Furthermore, AC knockdown and exogenous C16-ceramide supplementation induced similar changes in SF3B1 level and Mcl-1S/L ratio. Finally, we demonstrated that SACLAC treatment leads to a 37 to 75% reduction in leukemic burden in two human AML xenograft mouse models.

IMPLICATIONS

These data further emphasize AC as a therapeutic target in AML and define SACLAC as a potent inhibitor to be further optimized for future clinical development.

INTRODUCTION

Acute myeloid leukemia (AML) is a malignancy of the blood and bone marrow, characterized by uncontrolled proliferation of immature myeloid blasts. The current prognosis for most patients is poor, with 5-year survival at only 27% (1). AML is more common in older populations, with a median age of 68 at diagnosis. Unfortunately, older patients have even worse prognoses, with only 7% of patients over the age of 65 surviving 5 years past diagnosis (1–3). Patients generally receive a combination of general chemotherapeutics cytarabine (7 days) and daunorubicin (3 days) by continuous infusion. While new therapies have been approved recently, there is little change in overall survival. Some targeted therapies are available for patients with genetic mutations such as FLT3 and JAK2 (4), but AML is an extremely heterogeneous disease where the most recurrent genetic abnormality only exists in about 30% of patients (5–7). Treatment with FLT3 inhibitor quizartinib achieved about 50% composite complete remission for FLT3-ITD-positive patients, but only about 5% of patients achieved complete remission (8).

There is an urgent need for novel therapeutics in AML due to the limitations of current treatment options and poor patient survival (9,10), especially in the aging population that cannot tolerate intensive therapy (2,11). There are several hurdles involved in AML treatment, including therapy-related toxicity (12), genetic heterogeneity, *de novo* drug resistance and relapse (13). Identification of therapeutics that address these issues could greatly influence the future of AML treatment and improve patient prognosis.

An emerging area of study in cancer therapy involves manipulating sphingolipid metabolism in cancer cells to control cell fate (14). While sphingolipids are generally perceived as structural components of cellular membranes, there are two key bioactive sphingolipids at the center of this pathway. Ceramide is a known second messenger in cell death while sphingosine 1-phosphate (S1P) is pro-survival (15). Enzymes that mediate the conversion of ceramide to S1P are tightly regulated to maintain the balance between the integrity of healthy cells and the destruction of damaged cells. However, dysregulation of the enzymes regulating this pathway can contribute to many diseases including cancer (14,16,17). Acid ceramidase (ASAH1, referred to as AC) plays an important role in balancing these two lipids (17). AC is part of a family of lipid hydrolases that cleave ceramide to form sphingosine, which can be subsequently phosphorylated to produce S1P. AC is upregulated in several cancers (18–21). We recently established that it is the highest expressed and most upregulated ceramidase in AML and mediates survival of AML cells (22). We further demonstrated that elevated AC activity contributes to increased P-glycoprotein (P-gp) expression and a drug resistance phenotype in AML (23). Importantly, AC upregulation was observed in most AML patient samples, indicating that AC is a promising therapeutic target that may be applicable to a large percentage of AML patients.

We previously demonstrated that AC inhibition with LCL204 coincided with a loss of pro-survival Mcl-1 protein, leading to apoptosis (22). This finding is particularly relevant given the known importance of Bcl-2 family members in AML pathogenesis and

response to therapy (24). For example, upregulation of Mcl-1 is an established mechanism of resistance to the promising Bcl-2 inhibitor venetoclax, which is currently approved for use in elderly AML in combination with hypomethylating agents or low dose cytarabine (25–27). The full-length pro-survival Mcl-1 protein can also be referred to as Mcl-1L. However, Mcl-1 function can be altered through alternative mRNA splicing (28,29). When splicing is disrupted, exclusion of exon 2 results in formation of Mcl-1S. This step is regulated by SF3B1, a critical component of spliceosome assembly (28). Importantly, this alternative splicing event results in a dramatic change of function—Mcl-1L is pro-survival while Mcl-1S is pro-apoptotic (30). Mcl-1S retains the functional BH3 domain, which is critical for mitochondria-mediated induction of apoptosis (30,31). Previous studies have demonstrated that modulation of mRNA splicing can induce apoptosis of cancer cells (28,32).

Here, we utilize AC inhibition to increase ceramide levels and induce selective toxicity of AML cells. Further, we characterize a novel AC inhibitor to determine its efficacy and mechanism of action in AML cell lines, patient samples and xenograft models. By targeting AC, we aim to exploit a common biochemical dependence in AML cells that may represent a therapeutic approach that is broadly applicable to the diverse population of AML patients.

MATERIALS AND METHODS

Cell lines

Kasumi-1, Kasumi-3, Kasumi-6, ME-1, SET2 and SKM-1 cells were cultured in RPMI-1640 (Corning #10-040) with 20% FBS (VWR #97068-085). OCI-AML3 cells were cultured in RPMI-1640 with 15% FBS. OCI-AML4 cells were cultured in α-MEM (ThermoFisher #12571063) with 20% FBS and supplemented with 100 ng/ml hGM-CSF (Milltenyi Biotec #130-095-372). All KG1 derivative cells and OCI-M2 cells were cultured in IMDM (ThermoFisher #12440) with 20% FBS. All other cell lines were cultured in RPMI-1640 media supplemented with 10% FBS.

HL-60/VCR (33) cells were maintained in the presence of 1 µg/ml vincristine sulfate (Cayman #11764). HL-60/ABTR (34) cells were maintained in the presence of 5 µM ABT-737 (Cayman #11501). KG1/ABTR and KG1a/ABTR (34) cells were maintained in the presence of 1 µM ABT-737. Kasumi-6 and SNKO1 cells were supplemented with 10 ng/ml hGM-CSF. TF-1 cells were supplemented with 2 ng/ml hGM-CSF.

OCI-M2, SKNO1 and SKM-1 cell lines were obtained from DSMZ. All other cell lines were obtained from ATCC or kindly gifted according to the acknowledgements. All cells were grown at 37°C and 5% CO_2 in a humidified incubator. Cell lines were authenticated by short tandem repeat DNA profiling (Genetica DNA laboratories) and tested for mycoplasma contamination routinely using the MycoAlert PLUS detection kit (Lonza #LT07-710). Experiments were performed within 6 weeks of thawing.

HL-60/VCR, OCI-AML2 and THP-1 cell lines were chosen for characterization studies based on prevalence in literature and ease of maintenance. KG1a cells were chosen for siRNA studies based on transfection efficiency with published electroporation parameters. A table of RRID numbers for these cell lines can be found in the *Supplementary Appendix*.

AML patient samples

Samples were prepared from peripheral blood collected from newly diagnosed and untreated AML patients. Mononuclear cells were isolated by Ficoll-Paque (GE Healthcare Life Sciences) density gradient centrifugation. Cells were cultured in the serum-free medium StemSpan SFEM (referred to as SFEM) purchased from Stem Cell Technologies and supplemented with recombinant human stem cell factor (SCF, 100 ng/ml), interleukin-3 (IL-3, 20 ng/ml), FMS-like tyrosine kinase ligand (FLT3L, 100 ng/ml), granulocyte colony-stimulating factor (G-CSF, 20 ng/ml) and granulocyte-macrophage colony-stimulating factor (GM-CSF, 20 ng/ml) (Shenandoah Biotechnology). All cultures were incubated at 37°C with 5% CO_2. Informed consent was obtained from all patients under Penn State College of Medicine Institutional Review Board-approved protocol according to the Declaration of Helsinki.

Healthy donor samples

PBMCs from healthy donors were obtained from Virginia Blood Services and enriched using the Ficoll-Paque gradient separation method. $CD34^+$ PBMCs mobilized with G-

CSF were obtained from the University of Virginia Health System Blood Bank. $CD34^+$ cells were isolated from PBMCs with a Human CD34 MicroBead Kit (Miltenyi Biotec #130-046) using the autoMACS Pro Separator (Milltenyi Biotec #130-092-545).

Compounds

SACLAC *N*-[(2*S*,3*R*)-1,3-dihydroxyoctadecan-2-yl]2-chloroacetamide was synthesized as previously described (IQAC-CSIC) (35). The structure was validated using mass spectrometry. 2-Hydroxypropyl β-cyclodextrin was obtained from Acros Organics (#297561000). ABT-737 and ceramides mixture were obtained from Cayman Chemicals (#11501 and #22853, respectively). The ceramide mixture contained trace amount of C16 ceramide and varying amounts of longer chain and 2-hydroxy ceramides with C24 species being most abundant. C16 was purchased from Avanti Polar Lipids (#860516). All ceramides were dissolved in methanol with 2% dodecane. LCL204 was synthesized according to previously published methods (36). RBM14C12 substrate for AC activity assays was provided by Gemma Fabrias and Antonio Delgado (IQAC-CSIC).

Acid ceramidase activity assay

Cells were seeded at 2 x 10^4 cells per well in 50 µl. Acid ceramidase activity was measured at 24 hours using the RBM14C12 fluorogenic substrate as previously described (22,37).

Sphingolipid analysis

Lipid extraction and analysis was done using liquid chromatography-electrospray ionization-tandem mass spectrometry (LC-ESI-MS/MS) as previously described (22). Cells were plated at 5 million cells per 6 ml and treated with SACLAC or DMSO for 24 hours. Lipids were extracted from cell pellets using an azeotrophic mix of isopropanol:water:ethyl acetate (3:1:6; v:v:v). Internal standards (50 pmol of d17 long-chain bases and C12 acylated sphingolipids) were added to samples at the onset of the extraction procedure. Extracts were separated on a Waters I-class Acquity UPLC chromatography system. Mobile phases were (A) 60:40 water:acetonitrile and (B) 90:10 isopropanol:methanol with both mobile phases containing 5 mM ammonium formate and 0.1% formic acid. A Waters C18 CSH 2.1 mm ID × 10 cm column maintained at 65°C was used for the separation of the sphingoid bases, 1-phosphates, and acylated sphingolipids. The eluate was analyzed with an inline Waters TQ-S mass spectrometer using multiple reaction monitoring. All data reported are based on monoisotopic mass and are represented as pmol/mg protein.

Cell viability assay

For cell viability, cell lines were plated at 2.5 x 10^4 cells per well in a 96-well plate and treated with SACLAC or DMSO vehicle (0.4% of total volume) for the indicated time points and doses. At the experiment end point, 3-(4,5-Dimethylthiazol-2-yl)-5-(3-carboxymethoxyphenyl)-2-(4-sulfophenyl)-2H-tetrazolium (MTS) Cell Proliferation Colorimetric Assay Kit (BioVision # K300-5000) reagent was added and incubated for 2 hours. Conversion of MTS to formazan product was measured by absorbance at 490 nm using a BioTek Cytation 3 plate reader. Absorbance was normalized to DMSO control, which was defined as 100% viability. Due to limited cell numbers, patient

Author Manuscript Published OnlineFirst on November 19, 2019; DOI: 10.1158/1541-7786.MCR-19-0619
Author manuscripts have been peer reviewed and accepted for publication but have not yet been edited.

samples and normal samples were plated at $5x10^3$ cells per well in a 384-well plate with SACLAC or DMSO control for the indicated time points and doses. At the experiment end point, CellTiter-Glo Luminescent reagent (Promega #G7572) was added. After 15 minutes, luminescence was read on a BioTek Cytation 3 plate reader. Absorbance was normalized to DMSO control, which was defined as 100% viability.

Colony forming assay

Cryopreserved human AML patient samples were thawed and washed twice with RPMI 1640 supplemented with 2% heat inactivated fetal bovine serum (FBS). After washes, cells were cultured in triplicate in 12-well plates at a density of 0.1 to 2 x 10^5 cells per well in Human Methylcellulose Complete Media (R&D Systems, #HSC003). Plating densities were selected for each case to yield colony outgrowth of 20-100 colonies per well. The desired cell number and dose of SACLAC or DMSO was added to the culture media and dispensed to multi-well plates. Colonies were propagated for 10-14 days and blast colonies (>20 cells) were counted in a blinded manner under the light microscope.

Flow cytometry

Apoptosis in cell lines was assessed after treating 2.5 x 10^5 cells per ml with drug or vehicle in a 48-well plate for the indicated time points and doses. Primary human AML cells were pre-incubated with SFEM for 48 hours before plating 2 x 10^5 cells in 24-well plates for the indicated times point and doses. Samples were stained using the Muse Annexin V & Dead Cell Kit (Millipore #MCH100105). Change in mitochondrial membrane potential in cell lines was measured with the Muse MitoPotential Kit (Millipore #MCH100110). Caspase activation was measured using the Muse Caspase 3/7 Assay Kit (Millipore # MCH100108). For rescue experiments, cells were plated at 2.5 x 10^4 well in a 96-well plate 24 hours after electroporation. Cells were treated with DMSO or SACLAC for 48 hours and apoptosis was detected as stated above. All kits were used according to manufacturer's protocol. Cells were then analyzed using the Muse Cell Analyzer (38,39). Experiments included positive and negative controls for proper analysis.

Western blotting

Cells were plated at 2.5 x 10^5 cells per ml in 6-well plates and treated with drug, vehicle or siRNA at the indicated doses and time points. Cells were harvested, washed with PBS. Cells were lysed with RIPA buffer (Sigma #R0278) containing phosphatase inhibitor cocktails 2 and 3 (Sigma #P5726, #P0044) and protease inhibitor cocktail (Sigma #P8340). Protein was quantified using a bicinchoninic acid (BCA) protein assay kit (Pierce #23225). Samples were resolved on a Bolt 4-12% SDS-PAGE gel (ThermoFisher #NW00082) and transferred to PVDF membrane (Bio-Rad #170-4274). Antibodies were obtained from Cell Signaling Technology unless indicated otherwise. Primary antibodies used were: Mcl-1 (#5453, RRID #AB_10694494), SF3B1 (#14434, RRID #AB_2798479), β-actin (#3700, RRID #AB_2242334), Bim (#2819, RRID #AB_10692515) and AC (BD Biosciences #612302, RRID #AB_399617). Secondary antibodies used were HRP-linked goat anti-mouse (#7076, RRID #AB_330924) or goat anti-rabbit IgG (#7074, RRID #AB_2099233). Clarity Max Western ECL Substrate (Bio-Rad #1705062) was added to visualize relative protein expression by

chemiluminescence using the Bio-Rad ChemiDoc MP imaging system. Quantification was done using Bio-Rad ImageLab 6.0.1 software. For quantification, bands were normalized to β-actin as a loading control.

AC knockdown via siRNA electroporation or shRNA transduction

KG1a cells were electroporated with non-targeting scrambled siRNA (Dharmacon #D-001810-10-20), siRNA targeting *ASAH1* (Dharmacon #L-005228-03-0010) or *MCL-1S* (Dharmacon #CTM-481502) using the Neon Transfection System (Invitrogen) according to the manufacturer's protocol with the following parameters: 3 x 10^7 cells per ml, 1700 pulse voltage, and 20 ms pulse width for a single pulse. AC knockdown cells were harvested 48 hours after transfection for analysis by western blot. Mcl-1S knockdown cells were re-plated to 2.5 x 10^5 cells per ml and treated with SACLAC 24 hours after electroporation. Control- and SACLAC-treated cells were harvested 48 hours after SACLAC treatment, corresponding to 72 hours after electroporation. HL-60/VCR cells were transduced with vectors expressing shRNA to target AC or GFP control as previously described (23).

Overexpression with cDNA via electroporation

KG1a cells were electroporated with empty vector, an M98 vector containing Mcl-1 cDNA (NM_021960.4; Genecopoeia) or a pCMV vector containing a synthetic sequence for WT SF3B1 (40) using the same protocol listed above. The SF3B1 construct was sequence verified and the sequence of the codon-optimized coding region is available from the original authors.

Quantitative reverse transcription PCR

Cells were seeded at 2.5 x 10^5 cells per ml in 6-well plates and treated with DMSO or SACLAC for six hours. Cells were harvested and resuspended in TRIzol reagent (Invitrogen #15596026). RNA was isolated using Direct-zol RNA Miniprep Plus (Zymo Research #R2072) according to the manufacturer's protocol. RNA was quantified using the Take3 microplate and the pre-programmed RNA quantification protocol on the Gen5 software for the Cytation 3 plate reader (BioTek). DNase treatment and reverse transcription were done using the iScript gDNA Clear cDNA Synthesis Kit (Bio-Rad #1725035) in accordance with the manufacturer's protocol. The qPCR reaction contained iTaq Universal SYBR Green (Bio-Rad #1725122), 140 ng cDNA and primers specific for *HPRT* (Bio-Rad #100-25636), *B2M* (Bio-Rad #100-25636) and *MCL-1S* (Eurofins; forward, 5'-GAGGAGGACGAGTTGTACCG-3' and reverse, 5'-ACTCCACAAACCCATCCTTG-3') (41). This primer pair specifically amplifies Mcl-1 transcript variant 2 (MCL-1S) according to BLAST analysis. C_T values were normalized using *B2M* and *HPRT* housekeeping genes and transformed to $2^{-\Delta CT}$ and the DMSO control was set to 1.

***In vivo* AML xenograft model**

Maximum tolerated dose of SACLAC was determined in NOD-*scid* IL2Rgamma^{null} (NSG) mice (*n*=5; Jackson Laboratories). Mice were injected with SACLAC reconstituted in β-HPCD (IV) daily for 5 days at a dose of 5 mg/kg body weight, respectively. For pharmacokinetics studies, Swiss Webster mice (*n*=3; Charles River

Laboratories) were injected with SACLAC dissolved in DMSO (40 mg/kg body weight, intraperitoneally) or dissolved in β-HPCD (5 mg/kg body weight, via tail-vein injection). Mice were euthanized and blood was harvested at time points ranging from 0 to 48 hours. Serum concentration of SACLAC was measured by mass spectrometry quantification relative to SACLAC standard using the method referenced above.

To assess the efficacy of SACLAC in a transplantable human AML model, two cell line models were used. For the MV4-11 model, 2.5 x 10^6 luciferase (luc2)- and yellow fluorescent protein (YFP)-expressing MV4-11 cells (34) in HBSS were introduced into 6- to 8-week-old female NSG mice via tail-vein injections. After 10-12 days, engraftment was confirmed using bioluminescence imaging with the IVIS Lumina LT Series III imaging system (Perkin Elmer). Mice were equally randomized into two groups of three mice and treated with vehicle or SACLAC at 5 mg/kg/day five times per week for 18 total injections. At the end of the treatment, animals were euthanized and peripheral blood was collected for flow cytometry analysis.

For the U937 model, 1 x 10^4 luciferase and tdTomato-expressing U937 cells (Addgene #72486, kindly gifted by Kazuhiro Oka) in HBSS were introduced into 6- to 8-week-old female NSG mice via tail-vein injections. After six days, engraftment was confirmed as stated above. Mice were equally randomized into two groups of five mice and treated with vehicle or SACLAC at 5 mg/kg/day five times per week for 15 total injections. Animals were euthanized and bone marrow was collected for flow cytometry analysis.

Red blood cells (RBC) were lysed with RBC Lysis Buffer (BioLegend #420301) followed by cell surface staining with anti-human CD45 antibodies (BioLegend #304014, clone HI30) and 7-AAD (BioLegend #420404) to detect viable human white blood cells (WBC) using an LSR II flow cytometer and BD FACS Diva software at the Penn State College of Medicine Flow Cytometry Core. Viable cells were identified by gating on 7AAD-negative cells gated from singlets (SSC-A and FSC-W scales), after excluding the debris (SSC-A and FSC-A scales). Percentage of YFP, tdTomato or hCD45 positive cells was determined in FlowJo software (Becton Dickinson).

All animal studies were performed with IACUC approval (PRAMS201246746).

Statistical analysis

Significance between two treatment groups was determined by the two-tailed unpaired *t*-test using the GraphPad Prism 7.0 software. Data sets containing multiple comparison were corrected using the Holm-Sidak method. Experiments containing dose response or time courses were analyzed using one-way ANOVA with Dunnett's post-test to compare each condition to a single control. Cell line studies were repeated for three independent experiments, each with three or more technical replicates unless otherwise stated. One representative experiment is shown with error bars representing standard error of the mean (SEM).

RESULTS

Previously published literature validated AC as a therapeutic target in AML while utilizing the small molecule inhibitor LCL204, which is clinically limited by lysosomal toxicity (22). To further investigate the potential of AC inhibitors for AML treatment, we tested a novel inhibitor that binds irreversibly to AC.

SACLAC inhibits AC and shifts lipid levels toward a pro-death phenotype

SACLAC is an α-chloroamide ceramide analog (**Figure 1A**) that binds irreversibly to AC by transferring a covalent adduct to the enzyme catalytic site (35). We expected that inhibition of AC with SACLAC would cause accumulation of ceramides by blocking the breakdown of ceramide to sphingosine and further conversion to S1P. Three human AML cell lines were selected to evaluate SACLAC inhibition of AC activity in AML. The multidrug resistant HL-60/VCR cell line, which overexpresses P-gp (23) was treated alongside THP-1 and OCI-AML2 cell lines with SACLAC (2.5 μM). AC activity of these cell lines was reduced by 98%, 71% and 100%, respectively, with 24-hour treatment (**Figure 1B**). This is superior to LCL204, which requires a four-fold higher dose to achieve similar effects (**Figures S1**). We measured changes in S1P and ceramides under the same conditions. SACLAC reduced S1P content by 87% in HL-60/VCR and reduced S1P levels to below the limit of detection in THP-1 and OCI-AML2 cell lines (**Figure 1C**). Further, these conditions led to a 2- to 3-fold increase in total ceramide production (**Figure 1D**). Most individual ceramide species increased upon SACLAC treatment, with the most pronounced changes being C16, C18, C22:1 and C24:2 (**Figure S2**). Together these data indicate that SACLAC robustly inhibits AC activity and shifts lipid levels in the expected manner, increasing pro-death ceramides and decreasing pro-survival S1P.

SACLAC reduces viability and colony formation

Next, we determined if these shifts in lipid content were functionally significant and universally observed in human AML cell lines and patient samples. The same three representative cell lines were treated with SACLAC and cell viability was determined by MTS assay. HL-60/VCR, THP-1 and OCI-AML2, had half maximal inhibitory concentration (EC_{50}) values in the low-micromolar range (3.3, 2.6 and 1.8 μM, respectively) with 24-hour treatment (**Figure 2A**). To determine if this effect translated to AML patient cells, colony formation was analyzed in a panel of six primary patient samples. These six primary patient samples showed a reduced ability to form colonies in the presence of increasing doses of SACLAC. On average, colony formation decreased 32% with 5 μM treatment and 69% with 20 μM treatment (**Figure 2B**). Since AML is a heterogeneous disease, we assayed 30 human AML cell lines by MTS assay at 24 and 48-hour time points. Remarkably, 25 of 30 cell lines had EC_{50} values below 5 μM, with an average EC_{50} of 3.2 μM (**Figure 2C**). The outlier cell line OCI-M2 could be an interesting cell line to investigate further in the context of sphingolipid metabolism, AC and mechanisms of SACLAC action and/or resistance. SACLAC treatment for 24 hours slightly reduced normal cell viability. PBMCs (n=6) had an average EC_{50} of 7.4 μM while $CD34^+$ (n=4) cells averaged 4.0 μM (**Figure S3**). These data show that,

although there is variability in sensitivity, SACLAC is broadly toxic to AML cells with lesser toxicity in normal cells.

SACLAC induces apoptosis and loss of mitochondrial membrane potential

After confirming that SACLAC treatment reduced cell viability, the mechanism of cell death was examined. First, apoptosis induction was evaluated over time in OCI-AML2 cells treated with SACLAC (5 μM; **Figure 3A**). Apoptosis was induced as early as 12 hours (79% apoptosis) with nearly all cells undergoing apoptosis at 24 hours. Loss of mitochondrial membrane potential (**Figure 3B**) occurred in parallel with positive staining for the apoptosis marker annexin V (**Figure 3A**). These patterns were also observed in an additional cell line, THP-1 (**Figure S4A-B**). Additionally, dose-dependent caspase activation was observed with SACLAC treatment (**Figure 3C**). Three human AML cell lines exhibited dose-dependent induction of Annexin V staining with 48-hour SACLAC treatment, albeit with varying sensitivity (**Figure 3D**). AML patient samples exhibited similar results with more than half the samples reaching 80% apoptosis or greater with SACLAC treatment (**Figure 3E**). These data suggest that apoptosis is the predominant mechanism for SACLAC-induced cell death in AML cells.

SACLAC alters the ratio of pro-survival to pro-apoptotic Mcl-1 isoforms

Next, we investigated mechanisms that mediate apoptosis induction in SACLAC-treated OCI-AML2 cells after 24-hour exposure to increasing doses of SACLAC. Since Mcl-1 has been implicated in AML pathogenesis and specifically in response to sphingolipid modulation (22), changes in Mcl-1 with SACLAC treatment were examined. Most notably, SACLAC induced a 10-fold upregulation of the Mcl-1S isoform, which translated to a 3-fold increase in the ratio of pro-apoptotic Mcl-1S to pro-survival Mcl-1L (**Figure 4A,C**). Since changes in Mcl-1S were observed, splicing factors known to regulate Mcl-1 were also examined. SACLAC treatment reduced SF3B1 protein expression (**Figure 4A-B**), suggesting that spliceosome assembly and exon inclusion may be disrupted (42). Another splicing factor, SRSF1, was not affected (data not shown). Because Mcl-1 can also be cleaved by caspases to generate a smaller protein fragment, ABT-737-treated cells were used as a positive control for caspase-mediated Mcl-1 cleavage (43). ABT-737 treatment resulted in the expected smaller fragment of approximately 22 kDa that was abrogated by co-treatment with caspase inhibitor Z-VAD-FMK. However, SACLAC treatment led to the appearance of the larger Mcl-1S at about 32 kDa, which is the result of alternative mRNA splicing and was not blocked by caspase inhibitor treatment (**Figure 4D**). SF3B1 inhibition with Spliceostatin A (SSA) resulted in a dose-dependent increase in Mcl-1S (**Figure 4E**), which confirm SF3B1's role in Mcl-1 splicing in OCI-AML2 cells. Mcl-1 exon 2 exclusion was confirmed using RT-qPCR with primers specific for the Mcl-1S isoform. We observed increased MCL-1S transcript in OCI-AML2 cells treated with 5 μM SACLAC (**Figure 4F**). In order to determine if this mechanism is conserved across multiple AML cell lines, we examined changes in protein signaling after treating THP-1, HL60-VCR and KG1a cell lines with SACLAC for 48 hours. Similar to OCI-AML2 cells, SACLAC reduced SF3B1 levels and increased the pro-apoptotic ratio of Mcl-1S/L in all three cell lines (**Figure S4C-E**). The levels of Bim protein isoforms, which represent an alternative downstream readout of spliceosome function (44), were also shown to be altered in two cell lines upon

SACLAC treatment (**Figure S4C**). These observations implicate SF3B1 and Mcl-1S in SACLAC-mediated intrinsic apoptosis of AML cells.

C16 ceramide treatment and AC knockdown reduce SF3B1 and increase Mcl-1S/L ratio

In order to determine if ceramide is upstream of this mechanistic observation, three human AML cell lines were treated with a 100 µg/ml (~150 µM) mixture of ceramides, predominantly C18 species and longer. The ceramide mixture induced 60% apoptosis with 48-hour treatment (**Figure S5A**). Treatment with C16 ceramide (20 µM) induced similar levels of apoptosis (**Figure S5B**). Further, treatment with C16 ceramide induced similar mechanistic effects as SACLAC, with a reduction in SF3B1 and an increase in the ratio of Mcl-1S to Mcl-1L (**Figure 5A-C**). These data demonstrate that exogenous supplementation with ceramides that were shown to increase in response to SACLAC treatment (**Figure S3**) is sufficient to induce apoptosis and alternative Mcl-1 splicing in AML. To determine if SACLAC effects on AML cells are dependent on inhibition of AC activity, we knocked down AC protein using siRNA. Treatment of KG1a cells with siRNA targeting AC reduced AC protein by 76% at 48 hours post-transfection (**Figure 5D**). At this time point, SF3B1 was reduced 37% and the ratio of Mcl-1S to Mcl-1L increased by 83% (**Figure 5E-F**). We confirmed in an additional cell line, HL-60/VCR, that shRNA-mediated AC knockdown led to reduced SF3B1 protein levels, increased Mcl-1S expression and Mcl-1S/L ratio as well as altered Bim protein isoform abundance (**Figure S6**).

Altering expression of Mcl-1 and SF3B1 attenuates induction of apoptosis in SACLAC-treated cells

Next, we investigated the importance of Mcl-1S in the mechanism of SACLAC-mediated cell death. A custom siRNA was designed to target the junction of exons 1 and 3, which is present only in the MCL-1S transcript. KG1a cells were electroporated with this siRNA and treated with DMSO or SACLAC. Presence of short isoform-specific siRNA attenuated the induction of Mcl-1S protein expression upon SACLAC treatment (**Figure 6A)**. Further, apoptosis induction was reduced by 36% in SACLAC-treated Mcl-1S knockdown cells (**Figure 6D**). Next, we utilized cDNA expression vectors to overexpress MCL-1L (**Figure 6B)** or SF3B1 (**Figure 6C**) in KG1a cells. Each of these conditions led to a partial rescue of apoptosis in SACLAC-treated cells (**Figures 6E-F)**. Electroporation of expression vectors led to increased baseline apoptosis in KG1a cells (**Figure S7**). Therefore, the magnitude of SACLAC induced apoptosis after baseline subtraction is reduced in Figures 6E-F relative to Figure 6D. In summary, SACLAC treatment inhibits AC which leads to increased ceramide and decreased SF3B1. As ceramide accumulates, alternative splicing of Mcl-1 results in Mcl-1S accumulation that facilitates mitochondrial membrane depolarization. With loss of mitochondrial membrane potential ($\Delta\Psi m$), pro-apoptotic signals are released to activate caspases and induce apoptosis (**Figure S8**).

SACLAC reduces leukemic burden in NSG mouse models of AML

Ultimately, we wanted to determine if SACLAC treatment provides therapeutic benefit. We first confirmed that our maximum deliverable dose did not exceed a tolerable dose for the animals (data not shown). NOD-*scid* IL2Rgamma^{null} (NSG) immunodeficient mice were engrafted with human MV4-11 AML cells and then treated with 5 mg/kg SACLAC five times per week by tail-vein injection (**Figure 7A**). This dose and route of administration were chosen based upon studies indicating that IV delivery yields a higher maximal serum concentration than IP delivery (**Figure S9A**). SACLAC exhibited a short half-life in the blood (**Figure S9A**), yet levels of the sphingosine product were reduced in the liver for at least 6 hours after treatment (**Figure S9B**). After 18 injections, circulating leukemic cells in the blood were counted using flow cytometry. SACLAC treatment resulted in a significant (~75%) decrease in leukemic burden (**Figure 7B-C**). No overt toxicity was observed and SACLAC treated animals exhibited weight gain (data not shown). A second, more aggressive model using U937 AML cells (**Figure 7D**) exhibited up to 50% reduction in leukemic cells in the bone marrow of SACLAC-treated mice (**Figure 7E-F**). These data in two preclinical human AML xenograft models highlight the potential therapeutic efficacy of SACLAC in AML.

DISCUSSION

Here we determined that the AC inhibitor SACLAC kills cells via intrinsic apoptosis mediated through a signaling pathway that includes ceramide and Mcl-1S. We showed that SACLAC represents a promising compound for further optimization because it is broadly cytotoxic across AML cell lines and patient samples. Importantly, SACLAC treatment reduces leukemic burden in mice, even at nanomolar serum concentrations.

Our findings build upon previous reports that AC is an emerging therapeutic target that regulates the crucial balance between pro-survival S1P and pro-death ceramides (14,16,45,46). However, current studies targeting AC in AML are limited. Those that exist utilized inhibitors that have overt off-target effects (22) or require large doses for cytotoxicity (47). In contrast, SACLAC binds directly to the catalytic site of AC. Moreover, therapeutic effects were observed in murine xenograft models despite limited ability to deliver high doses of the compound. These *in vivo* models affirm that SACLAC is non-toxic at the administered therapeutic dose. However, *in vivo* delivery was limited by low solubility of the compound. While more work is clearly required to enhance the *in vivo* delivery and clinical potential of SACLAC, our studies present an important mechanistic characterization that will inform future optimization of this compound.

Our studies identify a novel association between AC inhibition and alternative splicing in AML. Mcl-1 protein is clearly associated with survival of AML cells (24). Mcl-1 and sphingolipids have been linked by previous work connecting Mcl-1 with AC (22), S1P (48), and ceramide signaling (49). However, these “traditional” relationships focused on changes in the full length Mcl-1 protein (Mcl-1L). In contrast, our studies highlight a unique mechanism whereby altered splicing leads to a pro-apoptotic Mcl-1 ratio. Importantly, this key role for Mcl-1S in SACLAC-mediated cell death is reinforced by a partial rescue of viability with knockdown of Mcl-1S as well as overexpression of Mcl-1 or SF3B1 (**Figure 6B,F**). These results suggest that alternative splicing of Mcl-1 cooperates with and compliments other major apoptotic contributors, such as ceramide accumulation, S1P depletion and diminished Mcl-1L, to enhance SACLAC-mediated cell death.

The relationship between SF3B1 and Mcl-1 has been established (28), and we also demonstrated modified protein isoform abundance for an additional target downstream of spliceosome function, Bim. The molecular mechanism whereby elevated ceramide and/or SACLAC levels lead to SF3B1 reduction is unclear. Ceramides may regulate SF3B1 expression through activation of protein phosphatase 1 (PP1) which is known to bind the RNA recognition motif of several splicing factors (50). Ongoing studies will more fully characterize these mechanisms as well as global changes in transcript splice variants, which may also identify factors that drive sensitivity to SACLAC or other sphingolipid targeting approaches.

Reduced SF3B1 levels and increased Mcl-1S/L ratios were observed consistently upon AC knockdown via both siRNA and shRNA, SACLAC treatment and ceramide supplementation (**Figures 4, 5 and S6**). The AC siRNA knockdown results differed

slightly in that loss of Mcl-1L was the major factor in the 2-fold increase of Mcl-1S to Mcl-1L compared to primarily increased Mcl-1S upon SACLAC or ceramide treatment and changes in both isoforms with AC shRNA. This difference is likely associated with variation in temporal dynamics and sphingolipid subcellular distribution associated with different types of manipulation. For example, AC activity loss will be more rapid and complete with inhibitor treatment relative to siRNA-mediated knockdown. Another likely contributor is the abundance of Mcl-1S and L isoforms in KG1a cells relative to other AML cell lines (**Figure S4C**). We previously reported loss of Mcl-1L upon LCL-204 treatment and AC knockdown in multiple human AML cell lines (22). LCL204 is known to induce lysosomal disruption that likely contributes to the proteasomal degradation of Mcl-1 observed in our previous studies, which did not investigate levels of Mcl-1S (22). These varying Mcl-1 alterations may relate to the diverse and complex regulatory mechanisms that control Mcl-1 transcription, stability and localization (22,51). Indeed, a reduction in Mcl-1L levels was also detected after SACLAC treatment in our studies with the exogenous overexpression of an Mcl-1L/EGFP fusion protein. Expanding our understanding of temporal and spatial relationships when utilizing sphingolipid modulators or sphingolipids themselves, as well as the downstream effects on Mcl-1, will enhance future therapeutic targeting of sphingolipid metabolism.

The observed changes in SF3B1 and Mcl-1 are particularly interesting since a subset of the common somatic mutations in AML involve genes that regulate RNA binding and spliceosome assembly (52). Interestingly, myelodysplastic syndrome (MDS), which sometimes precedes AML, exhibits spliceosome mutations in about 50% of cases and responds noticeably well to spliceosomal inhibition (32). Additional clinical relevance of our studies is highlighted by Mcl-1's known role in resistance to Bcl-2 inhibitor venetoclax (ABT-199) (25,53). Venetoclax was recently granted breakthrough status for the treatment of newly diagnosed AML in combination with hypomethylating agents or low dose cytarabine (54,55). Because of its ability to transition Mcl-1 from pro-survival to pro-apoptotic isoforms, SACLAC combination may further enhance the efficacy of venetoclax in AML patients and other cancers. SACLAC may also be more beneficial than Mcl-1 specific inhibitors in combination therapies due to its pro-apoptotic conversion of sphingolipid levels. Ongoing studies in our lab are exploring the relative efficacy of SACLAC combinatorial treatments.

The primary limitation for *in vivo* studies was the poor solubility and limited uptake of SACLAC. We were able to improve delivery of SACLAC by changing administration route and vehicle (**Figure S9A**), but only achieved peak serum SACLAC levels of less than 1 μM. The control and SACLAC-treated mice were of similar health at termination of the study. Nonetheless, we observed significant differences in leukemic burden at the cellular level. Identifying improved solvents, alternative formulations or structural derivatives of SACLAC may improve therapeutic efficacy. SACLAC-treated mice did not lose weight over the course of the study. Future studies will continue to carefully evaluate normal bone marrow toxicity as increased SACLAC delivery is achieved.

Our findings are especially important because of AML patient heterogeneity (5). While mutation-targeted therapeutics are best suited for specific patient subpopulations,

SACLAC appears to exploit a common biochemical dependence across the vast majority of AML cell lines and patient samples. While AC upregulation and ceramide mediated apoptosis have been established previously (22), we have advanced this field by characterizing a novel inhibitor with a unique mechanism of action (**Figure 4**) and *in vivo* efficacy (**Figure 7**). Additionally, our screen of 30 AML cell lines represents the largest panel of AC inhibitor efficacy studies in AML to date. Further, these studies elucidate the mechanism of SACLAC cytotoxicity in AML cells and inform future efforts to design combination therapies or combat potential resistance.

Our data support the involvement of AC, ceramide, SF3B1 and Mcl-1 in SACLAC-mediated apoptosis. However, we cannot completely rule out the possibility of off-target or bi-phasic effects of SACLAC. Changes in AC activity, lipid levels and cell viability were detected at slightly lower doses than those required to induce robust apoptosis. This could mean that cells have a threshold or short-term tolerance for these changes upon low dose SACLAC treatment. At higher SACLAC doses, it is plausible that additional sphingolipid changes and/or elevated SACLAC levels further increase the alterations in SF3B1 and Mcl-1, which cooperate with ceramide accumulation to enhance apoptosis induction. Correlation analysis did not identify a significant relationship between SACLAC EC_{50} value and AC enzymatic activity within the 30 cell lines. Therefore, SACLAC sensitivity is not simply associated with the levels of the enzymatic target. This is likely attributed to the cell line-specific uptake, transport and localization of SACLAC (itself a ceramide analog) and sphingolipids as well as the varied, cell line-specific biochemical flux within each portion of the complex sphingolipid synthesis, catalysis and conversion pathways. Future studies will explore the predictors and regulators of SACLAC sensitivity.

Together, our studies demonstrate that ceramide accumulation leading to SF3B1 reduction and Mcl-1S induction is a primary mechanism of action for novel inhibitor SACLAC. Our findings highlight the role of AC and sphingolipids in AML and identify SACLAC as a novel compound that informs ongoing lipid-based targeting strategies in AML.

ACKNOWLEDGMENTS

The authors thank those who generously provided cell lines for our studies: Dr. Jacqueline Cloos and Carolien van Alphen, VU Medical Center Amsterdam (EOL-1, HEL, Kasumi-3, Kasumi-6, ME-1, ML2, MM-6 and NB4); Dr. Mark Levis, Johns Hopkins Medical Institutions (MOLM-13 and MOLM-14); Dr. Douglas Graham, Emory University (NOMO1); Dr. Xiaorong Gu, Cleveland Clinic (OCI-AML2 and OCI-AML3); Dr. Harold L. Atkins, Ottawa Hospital Research Institute (OCI-AML4); Drs. Scott Kaufmann and Mithun Shah, Mayo Clinic (SET2); and Barbara Miller, Penn State Hershey (U937-Luc2-P2A-tdTomato).

The authors also thank Alex Wendling, Wendy Dunton, Emily Sullins, Matthew Schmachtenberg and Shubha Dighe (University of Virginia) and Viola Devine (Penn State Hershey) for technical assistance, Tye Deering (University of Virginia) for his lipid expertise, and Antonio Delgado (IQAC-CSIC) for SACLAC and RBM14C12 synthesis. The authors thank Marieke Jones (University of Virginia) for her statistics expertise. The authors thank the staff of the Flow Cytometry Core at Penn State University College of Medicine (Hershey, PA). The authors thank Drs. Melissa Jurica and Arun Ghosh (University of California, Santa Cruz) for providing spliceostatin A for these studies. The authors also thank Drs. Samar Alsafadi and Marc-Henri Stern (Curie Institute) for providing the vector for SF3B1 overexpression.

This work was supported by the National Institutes of Health under the National Cancer Institute Award Number P01CA171983 (to TP Loughran and M Kester), P30CA044579 (to TP Loughran) and under the National Institute of General Medicine Sciences Award Number T32GM007055 (to JM Pearson) and AEI/FEDER Grant Number CTQ2017-85378-R (to G Fabrias). The content is solely the responsibility of the authors and does not necessarily represent the official views of the National Institutes of Health. Additional funding was provided to TP Loughran by the Bess Family Charitable Fund and a generous anonymous donor.

REFERENCES

1. Noone A, Howlader N, Krapcho M, Miller D, Brest A, Yu M, et al. SEER Cancer Statistics Review, 1975-2015 [Internet]. Natl. Cancer Inst. [cited 2018 Sep 4]. Available from: https://seer.cancer.gov/csr/1975_2015/

2. Klepin HD, Balducci L. Acute Myelogenous Leukemia in Older Adults. The Oncologist. 2009;14:222–32.

3. Dombret H, Gardin C. An update of current treatments for adult acute myeloid leukemia. Blood. 2016;127:53–61.

4. Hatzimichael E, Georgiou G, Benetatos L, Briasoulis E. Gene mutations and molecularly targeted therapies in acute myeloid leukemia. Am J Blood Res. 2013;3:29–51.

5. Martelli MP, Sportoletti P, Tiacci E, Martelli MF, Falini B. Mutational landscape of AML with normal cytogenetics: biological and clinical implications. Blood Rev. 2013;27:13–22.

6. Tyner JW, Tognon CE, Bottomly D, Wilmot B, Kurtz SE, Savage SL, et al. Functional genomic landscape of acute myeloid leukaemia. Nature. 2018;562:526–31.

7. Cancer Genome Atlas Research Network, Ley TJ, Miller C, Ding L, Raphael BJ, Mungall AJ, et al. Genomic and epigenomic landscapes of adult de novo acute myeloid leukemia. N Engl J Med. 2013;368:2059–74.

8. Cortes J, Perl AE, Döhner H, Kantarjian H, Martinelli G, Kovacsovics T, et al. Quizartinib, an FLT3 inhibitor, as monotherapy in patients with relapsed or refractory acute myeloid leukaemia: an open-label, multicentre, single-arm, phase 2 trial. Lancet Oncol. 2018;19:889–903.

9. Wiese M, Daver N. Unmet clinical needs and economic burden of disease in the treatment landscape of acute myeloid leukemia. Am J Manag Care. 2018;24:S347–55.

10. Hong W-J, Medeiros BC. Unfavorable-risk cytogenetics in acute myeloid leukemia. Expert Rev Hematol. 2011;4:173–84.

11. Papaemmanuil E, Gerstung M, Bullinger L, Gaidzik VI, Paschka P, Roberts ND, et al. Genomic Classification and Prognosis in Acute Myeloid Leukemia. N Engl J Med. 2016;374:2209–21.

12. Buckley SA, Othus M, Estey EH, Walter RB. The treatment-related mortality score is associated with non-fatal adverse events following intensive AML induction chemotherapy. Blood Cancer J. 2015;5:e276.

13. Burrell RA, Swanton C. Tumour heterogeneity and the evolution of polyclonal drug resistance. Mol Oncol. 2014;8:1095–111.

14. Ryland LK, Fox TE, Liu X, Loughran TP, Kester M. Dysregulation of sphingolipid metabolism in cancer. Cancer Biol Ther. 2011;11:138–49.

15. Takabe K, Spiegel S. Export of sphingosine-1-phosphate and cancer progression. J Lipid Res. 2014;55:1839–46.

16. Morad SAF, Cabot MC. Ceramide-orchestrated signalling in cancer cells. Nat Rev Cancer. 2013;13:51–65.

17. Mao C, Obeid LM. Ceramidases: regulators of cellular responses mediated by ceramide, sphingosine, and sphingosine-1-phosphate. Biochim Biophys Acta. 2008;1781:424–34.

18. Camacho L, Meca-Cortés O, Abad JL, García S, Rubio N, Díaz A, et al. Acid ceramidase as a therapeutic target in metastatic prostate cancer. J Lipid Res. 2013;54:1207–20.

19. Leclerc J, Garandeau D, Pandiani C, Gaudel C, Bille K, Nottet N, et al. Lysosomal acid ceramidase ASAH1 controls the transition between invasive and proliferative phenotype in melanoma cells. Oncogene. 2019;38.

20. Flowers M, Fabriás G, Delgado A, Casas J, Abad JL, Cabot MC. C6-ceramide and targeted inhibition of acid ceramidase induce synergistic decreases in breast cancer cell growth. Breast Cancer Res Treat. 2012;133:447–58.

21. Nguyen H, Awad A, Shabani S, Doan N, Nguyen HS, Awad AJ, et al. Molecular Targeting of Acid Ceramidase in Glioblastoma: A Review of Its Role, Potential Treatment, and Challenges. Pharmaceutics. 2018;10:45.

22. Tan S-F, Liu X, Fox TE, Barth BM, Sharma A, Turner SD, et al. Acid ceramidase is upregulated in AML and represents a novel therapeutic target. Oncotarget. 2016;7:83208–22.

23. Tan S-F, Dunton W, Liu X, Fox TE, Morad SAF, Desai D, et al. Acid ceramidase promotes drug resistance in acute myeloid leukemia through NF-kB-dependent P-glycoprotein upregulation. J Lipid Res. 2019;60:1078–86.

24. Glaser SP, Lee EF, Trounson E, Bouillet P, Wei A, Fairlie WD, et al. Anti-apoptotic Mcl-1 is essential for the development and sustained growth of acute myeloid leukemia. Genes Dev. 2012;26:120–5.

25. Luedtke DA, Niu X, Pan Y, Zhao J, Liu S, Edwards H, et al. Inhibition of Mcl-1 enhances cell death induced by the Bcl-2-selective inhibitor ABT-199 in acute myeloid leukemia cells. Signal Transduct Target Ther. 2017;2:17012.

26. Teh T-C, Nguyen N-Y, Moujalled DM, Segal D, Pomilio G, Rijal S, et al. Enhancing venetoclax activity in acute myeloid leukemia by co-targeting MCL1. Leukemia. 2018;32:303–12.

27. Aldoss I, Yang D, Aribi A, Ali H, Sandhu K, Al Malki MM, et al. Efficacy of the combination of venetoclax and hypomethylating agents in relapsed/refractory acute myeloid leukemia. Haematologica. 2018;103:e404–7.

28. Gao Y, Koide K. Chemical perturbation of Mcl-1 pre-mRNA splicing to induce apoptosis in cancer cells. ACS Chem Biol. 2013;8:895–900.

29. Morciano G, Giorgi C, Balestra D, Marchi S, Perrone D, Pinotti M, et al. Mcl-1 involvement in mitochondrial dynamics is associated with apoptotic cell death. Mol Biol Cell. 2016;27:20–34.

30. Bae J, Leo CP, Hsu SY, Hsueh AJW. MCL-1S, a Splicing Variant of the Antiapoptotic BCL-2 Family Member MCL-1, Encodes a Proapoptotic Protein Possessing Only the BH3 Domain. J Biol Chem. 2000;275:25255–61.

31. Chittenden T. BH3 domains: intracellular death-ligands critical for initiating apoptosis. Cancer Cell. 2002;2:165–6.

32. Lee SC-W, Abdel-Wahab O. Therapeutic targeting of splicing in cancer. Nat Med. 2016;22:976–86.

33. McGrath T, Latoud C, Arnold ST, Safa AR, Felsted RL, Center MS. Mechanisms of multidrug resistance in HL60 cells. Analysis of resistance associated membrane proteins and levels of mdr gene expression. Biochem Pharmacol. 1989;38:3611–9.

34. Doi K, Liu Q, Gowda K, Barth BM, Claxton D, Amin S, et al. Maritoclax induces apoptosis in acute myeloid leukemia cells with elevated Mcl-1 expression. Cancer Biol Ther. 2014;15:1077–86.

35. Ordóñez YF, Abad JL, Asseri M, Casas J, Garcia V, Casasampere M, et al. Activity-based imaging of acid ceramidase. J Am Chem Soc. 2019;

36. Bai A, Szulc ZM, Bielawski J, Mayroo N, Liu X, Norris J, et al. Synthesis and bioevaluation of ω-N-amino analogs of B13. Bioorg Med Chem. 2009;17:1840–8.

37. Gouazé-Andersson V, Flowers M, Karimi R, Fabriàs G, Delgado A, Casas J, et al. Inhibition of acid ceramidase by a 2-substituted aminoethanol amide synergistically sensitizes prostate cancer cells to N-(4-hydroxyphenyl) retinam... - PubMed - NCBI. The Prostate. 2011;71:1064–73.

38. Daniele S, Taliani S, Da Pozzo E, Giacomelli C, Costa B, Trincavelli ML, et al. Apoptosis Therapy in Cancer: The First Single-molecule Co-activating p53 and the Translocator Protein in Glioblastoma. Sci Rep. 2014;4.

39. Ru Q, Li W, Xiong Q, Chen L, Tian X, Li C-Y. Voltage-gated potassium channel blocker 4-aminopyridine induces glioma cell apoptosis by reducing expression of microRNA-10b-5p. Mol Biol Cell. 2018;29:1125–36.

40. Alsafadi S, Houy A, Battistella A, Popova T, Wassef M, Henry E, et al. Cancer-associated *SF3B1* mutations affect alternative splicing by promoting alternative branchpoint usage. Nat Commun. 2016;7:10615.

41. Crews LA, Balaian L, Delos Santos NP, Leu HS, Court AC, Lazzari E, et al. RNA Splicing Modulation Selectively Impairs Leukemia Stem Cell Maintenance in Secondary Human AML. Cell Stem Cell. 2016;19:599–612.

42. Dolatshad H, Pellagatti A, Fernandez-Mercado M, Yip BH, Malcovati L, Attwood M, et al. Disruption of SF3B1 results in deregulated expression and splicing of key genes and pathways in myelodysplastic syndrome hematopoietic stem and progenitor cells. Leukemia. 2015;29:1798.

43. Ryu Y, Hall CP, Reynolds CP, Kang MH. Caspase-dependent Mcl-1 cleavage and effect of Mcl-1 phosphorylation in ABT-737-induced apoptosis in human acute lymphoblastic leukemia cell lines. Exp Biol Med Maywood NJ. 2014;239:1390–402.

44. Ten Hacken E, Valentin R, Regis FFD, Sun J, Yin S, Werner L, et al. Splicing modulation sensitizes chronic lymphocytic leukemia cells to venetoclax by remodeling mitochondrial apoptotic dependencies. JCI Insight. 2018;3.

45. Tan SF, Pearson JM, Feith DJ, Loughran TP. The emergence of acid ceramidase as a therapeutic target for acute myeloid leukemia. Expert Opin Ther Targets. 2017;21:583–90.

46. Coant N, Sakamoto W, Mao C, Hannun YA. Ceramidases, roles in sphingolipid metabolism and in health and disease. Adv Biol Regul. 2017;63:122–31.

47. Morad SAF, Tan S-F, Feith DJ, Kester M, Claxton DF, Loughran TP, et al. Modification of sphingolipid metabolism by tamoxifen and N-desmethyltamoxifen in acute myelogenous leukemia – Impact on enzyme activity and response to cytotoxics. Biochim Biophys Acta. 2015;1851:919–28.

48. Powell JA, Lewis AC, Zhu W, Toubia J, Pitman MR, Wallington-Beddoe CT, et al. Targeting sphingosine kinase 1 induces MCL1-dependent cell death in acute myeloid leukemia. Blood. 2017;129:771–82.

49. Lin C-F, Tsai C-C, Huang W-C, Wang Y-C, Tseng P-C, Tsai T-T, et al. Glycogen Synthase Kinase-3β and Caspase-2 Mediate Ceramide- and Etoposide-Induced Apoptosis by Regulating the Lysosomal-Mitochondrial Axis. Zhivotovsky B, editor. PLOS ONE. 2016;11:e0145460.

50. Massiello A, Chalfant CE. SRp30a (ASF/SF2) regulates the alternative splicing of caspase-9 pre-mRNA and is required for ceramide-responsiveness. J Lipid Res. 2006;47:892–7.

51. Thomas LW, Lam C, Edwards SW. Mcl-1; the molecular regulation of protein function. FEBS Lett. 2010;584:2981–9.

52. Makishima H, Visconte V, Sakaguchi H, Jankowska AM, Abu Kar S, Jerez A, et al. Mutations in the spliceosome machinery, a novel and ubiquitous pathway in leukemogenesis. Blood. 2012;119:3203–10.

53. Wang Q, Wan J, Zhang W, Hao S. MCL-1 or BCL-xL-dependent resistance to the BCL-2 antagonist (ABT-199) can be overcome by specific inhibitor as single agents and in combination with ABT-199 in acute myeloid leukemia cells. Leuk Lymphoma. 2019;1–11.

54. Wei A, Strickland SA, Hou J-Z, Fiedler W, Lin TL, Walter RB, et al. Venetoclax with Low-Dose Cytarabine Induces Rapid, Deep, and Durable Responses in Previously Untreated Older Adults with AML Ineligible for Intensive Chemotherapy. Blood. 2018;132:284–284.

55. DiNardo CD, Pratz K, Pullarkat V, Jonas BA, Arellano M, Becker PS, et al. Venetoclax combined with decitabine or azacitidine in treatment-naive, elderly patients with acute myeloid leukemia. Blood. 2019;133:7–17.

FIGURE LEGENDS

Figure 1. SACLAC inhibits AC and shifts lipid levels toward a pro-death phenotype. A) SACLAC is an α-chloroamide ceramide analog. **B)** Acid ceramidase activity levels were measured by fluorogenic substrate conversion to determine AC inhibition after SACLAC (2.5 μM) treatment of HL-60/VCR, THP-1 and OCI-AML2 human AML cell lines for 24 hours. This experiment was repeated two to three times per cell line, and a representative experiment is shown. **C)** Sphingosine 1-phosphate and **D)** total ceramide levels were measured by mass spectrometry and normalized to total protein to determine sphingolipid changes in response to SACLAC (2.5 μM) treatment of human AML cell lines for 24 hours. This experiment contained five biological replicates and multiple doses with similar response. Statistical analysis was done using two-tailed unpaired t-test to compare DMSO and treatment. Lipid data was corrected for multiple testing using the Holm-Sidak method. * $p < 0.05$, ** $p < 0.01$, *** $p < 0.001$ relative to DMSO control. N.D. indicates values were below the limit of detection.

Figure 2. SACLAC reduces cell viability and colony formation. A) Viability of three human AML cell lines was measured by MTS assay after 24-hour treatment with the indicated dose of SACLAC. **B)** Colony formation assay measured clonogenic potential in a panel of six primary AML patient samples with increasing doses of SACLAC. This experiment contained six distinct patient samples as biological replicates. **C)** The concentration of SACLAC required to achieve a 50% reduction in cell viability (EC_{50}) in 30 different human AML cell lines was measured by MTS at 24 and 48 hours. Each dot represents one MTS assay (n=2-6). Global p-value (ANOVA) is presented on the graph. Asterisks denote pairwise comparison from Dunnett's Test comparing each dose to DMSO control. ** $p < 0.01$, *** $p < 0.001$.

Figure 3. SACLAC induces apoptosis and loss of mitochondrial membrane potential. OCI-AML2 cells were treated with DMSO or SACLAC (5 μM) and evaluated for **A)** apoptosis and **B)** mitochondrial membrane depolarization at the indicated time. **C)** Caspase 3/7 activation was determined in OCI-AML2 cells treated with increasing doses of SACLAC for 24 hours. Dose-dependent apoptosis was measured in **D)** human AML cell lines and **E)** primary patient samples with 48-hour SACLAC treatment (μM). Studies of patient samples were performed once with a panel of seven distinct patient samples and the line represents the group mean. Global p-value (ANOVA) is presented on the graph. Asterisks denote pairwise comparison from Dunnett's Test. Dose responses are compared to DMSO and time courses are compared to 0-hour time point. * $p < 0.05$, ** $p < 0.01$, *** $p < 0.001$.

Figure 4. SACLAC reduces expression of SF3B1 and increases pro-apoptotic Mcl-1S. A) OCI-AML2 cells were treated with the indicated dose of SACLAC for 24 hours, then SF3B1, Mcl-1S and Mcl-1L protein expression was measured by western blot. **B)** SF3B1 and **C)** Mcl-1S/L ratio were quantified relative to β-actin loading control and compared to DMSO vehicle control. **D)** Alternative splicing of Mcl-1 in OCI-AML2 cells treated for 24 hours with SACLAC (5 μM) was clearly distinguished from proteolytic cleavage of Mcl-1 induced by ABT-737 (75 nM) as a positive control. Appearance of the

Mcl-1 cleavage product, but not Mcl-1S, was blocked by caspase inhibitor Z-VAD-FMK (50 μM). **E)** SF3B1 involvement in Mcl-1 splicing was confirmed using 5 (+), 10 (++) or 20 nM (+++) spliceostatin A (SSA) to treat OCI-AML2 cells for 6 hours. This experiment was repeated twice. **F)** *MCL-1S* transcript levels after 6-hour treatment with 5 μM SACLAC were measured using RT-qPCR. This experiment was repeated twice. Global *p*-value (ANOVA) is presented on the graph. Asterisks denote pairwise comparison from Dunnett's Test comparing each dose to DMSO control. RT-qPCR analysis utilized two-tailed unpaired t-test to compare DMSO and treatment. * $p < 0.05$, ** $p < 0.01$, *** $p < 0.001$. SAC, SACLAC; VAD, Z-VAD-FMK; ABT, ABT-737; SSA, spliceostatin A.

Figure 5. C16 ceramide treatment and AC knockdown reduce SF3B1 and alter Mcl-1S to L ratio. A) SF3B1, Mcl-1L and Mcl-1S protein expression was measured by western blot after treatment with 20 μM C16 ceramide for 48 hours in OCI-AML2 human AML cells. **B)** SF3B1 and **C)** Mcl-1S/L ratio were quantified relative to β-actin loading control and compared to DMSO vehicle control. **D)** KG1a cells were electroporated with siRNA (50 nM) targeting AC and harvested 48 hours later. Knockdown was confirmed and changes in protein levels were evaluated using western blotting. Change in **E)** SF3B1 level and **F)** Mcl-1S/L ratio were quantified relative to scrambled siRNA as the control. Statistical analysis was done using two-tailed unpaired t-test to compare control (vehicle or scrambled siRNA) and treatment (C16 or targeting siRNA). * $p < 0.05$, ** $p < 0.01$.

Figure 6. Altering expression of Mcl-1 and SF3B1 attenuates induction of apoptosis in SACLAC-treated cells. A) KG1a cells were electroporated with custom siRNA (100 nM) targeting the *MCL-1S* transcript. After 24 hours, cells were treated with 10 μM SACLAC and analyzed by western blot for Mcl-1S protein expression 48 hours later. **B)** Mcl-1L and **C)** SF3B1 were overexpressed in KG1a cells by electroporating with 15 μg plasmid cDNA and then treated with 7.5 μM SACLAC, respectively, 24 hours later. Protein quantification is shown relative to DMSO control following normalization to β-actin. Mcl-1L is expressed as an Mcl-1/EGFP fusion protein in **B**; therefore, no quantitation is provided in empty vector lanes. The ability of **D)** Mcl-1S knockdown, **E)** Mcl-1L overexpression and **F)** SF3B1 overexpression to rescue cells from SACLAC mediated cell death was measured by comparing apoptosis induction over baseline (apoptosis in DMSO control group) for each condition. Overexpression experiments were repeated twice with two doses showing similar results. Statistical analysis utilized two-tailed unpaired t-test to compare control (scrambled siRNA or empty vector) and treatment (targeting siRNA or cDNA). ** $p < 0.01$, *** $p < 0.001$. Lines in blots indicate non-adjacent lanes on a single blot at the same exposure.

Figure 7. SACLAC reduces leukemic burden in NSG mouse models of AML. A) NOD-*scid* IL2Rgamma^{null} (NSG) mice (n=3 per group) were injected with 2.5x10^6 human MV4-11 cells labeled with YFP-Luc, and engraftment was confirmed by bioluminescence imaging after two weeks. Each animal received five tail-vein injections per week of SACLAC (5 mg/kg SACLAC in 45% w/v 2-hydroxypropyl-β-cyclodextrin in PBS) or vehicle control. After 18 injections, leukemic burden was measured in blood by flow cytometry staining for **B)** hCD45 and **C)** YFP markers to identify MV4-11 cells. **D)**

NSG mice (*n*=5 per group) were injected with $1x10^4$ human U937 cells labeled with tdTomato-Luc, and engraftment was confirmed by bioluminescence imaging after one week. Each animal received five tail-vein injections per week of SACLAC (5 mg/kg SACLAC in 45% w/v 2-hydroxypropyl-β-cyclodextrin in PBS) or vehicle control. After 15 injections, leukemic burden was measured by flow cytometry staining for **E)** hCD45 and **F)** tdTomato markers to identify U937 cells in bone marrow. Statistical analysis utilized two-tailed unpaired t-test to compare vehicle and SACLAC treatment. * $p < 0.05$.

Figure 1. SACLAC inhibits AC and shifts lipid levels toward a pro-death phenotype.

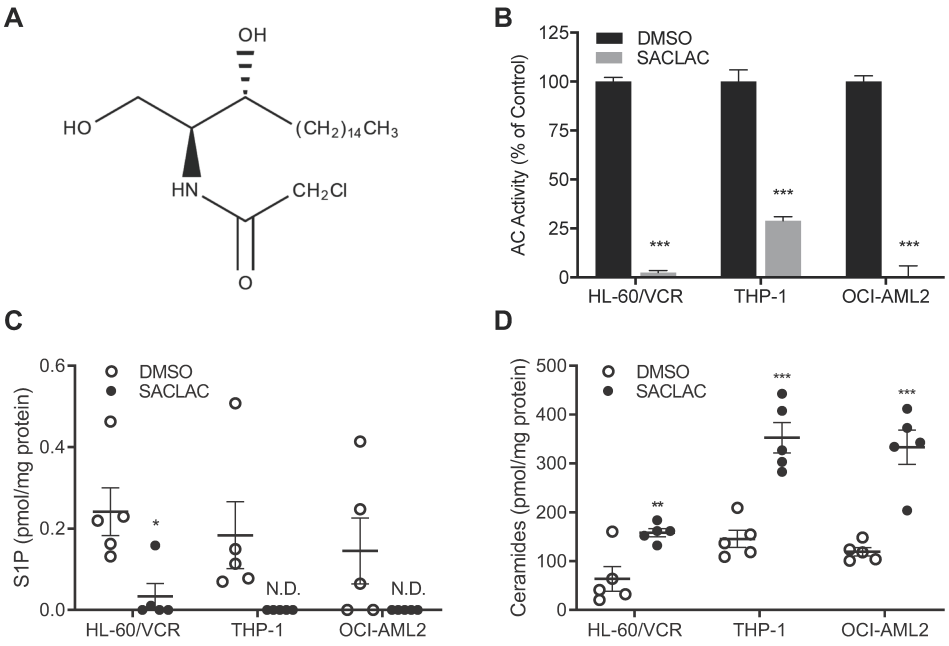

Figure 2. SACLAC reduces cell viability and colony formation.

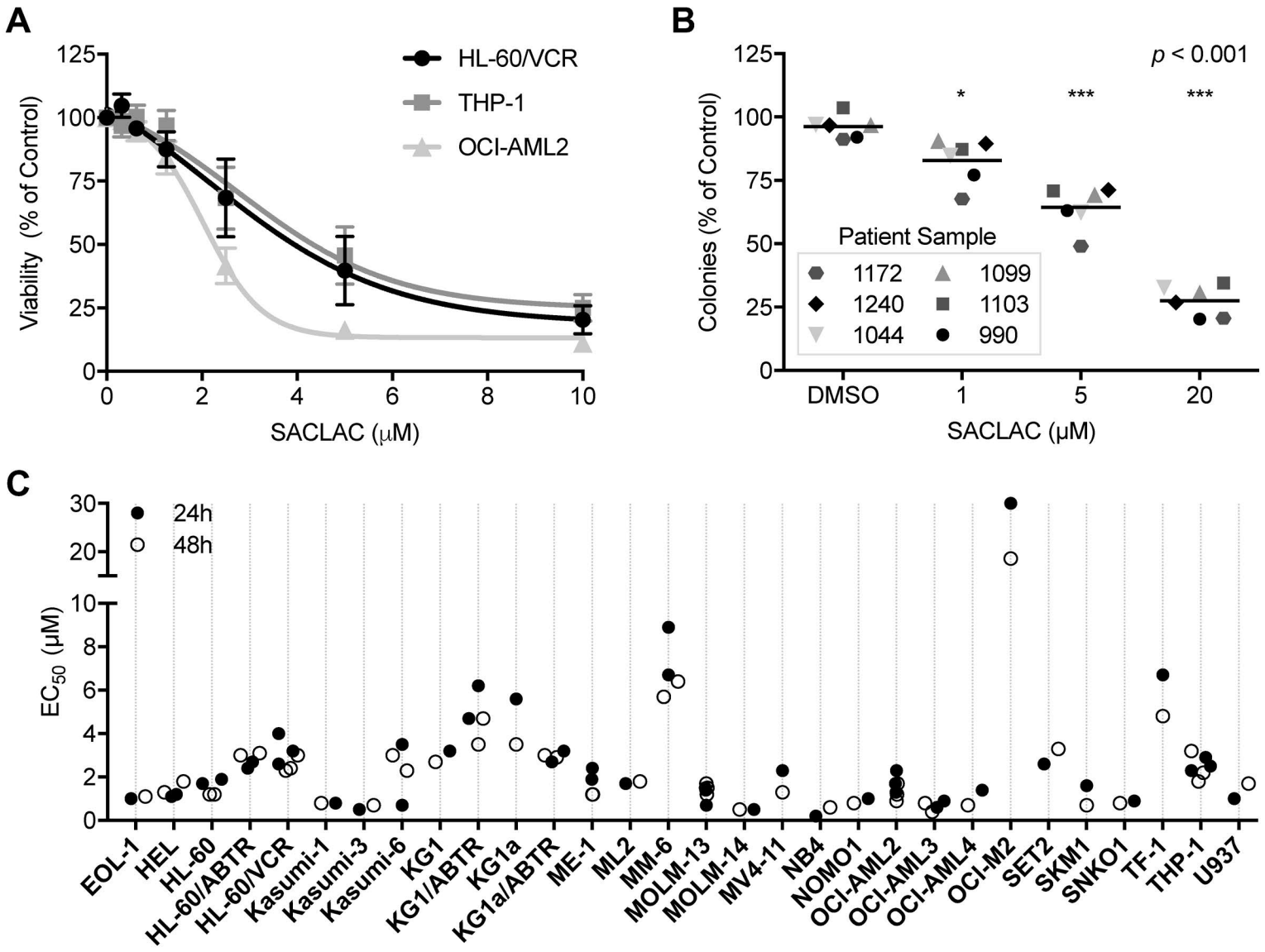

Author Manuscript Published OnlineFirst on November 19, 2019; DOI: 10.1158/1541-7786.MCR-19-0619
Author manuscripts have been peer reviewed and accepted for publication but have not yet been edited.

Figure 3. SACLAC induces apoptosis and loss of mitochondrial membrane potential.

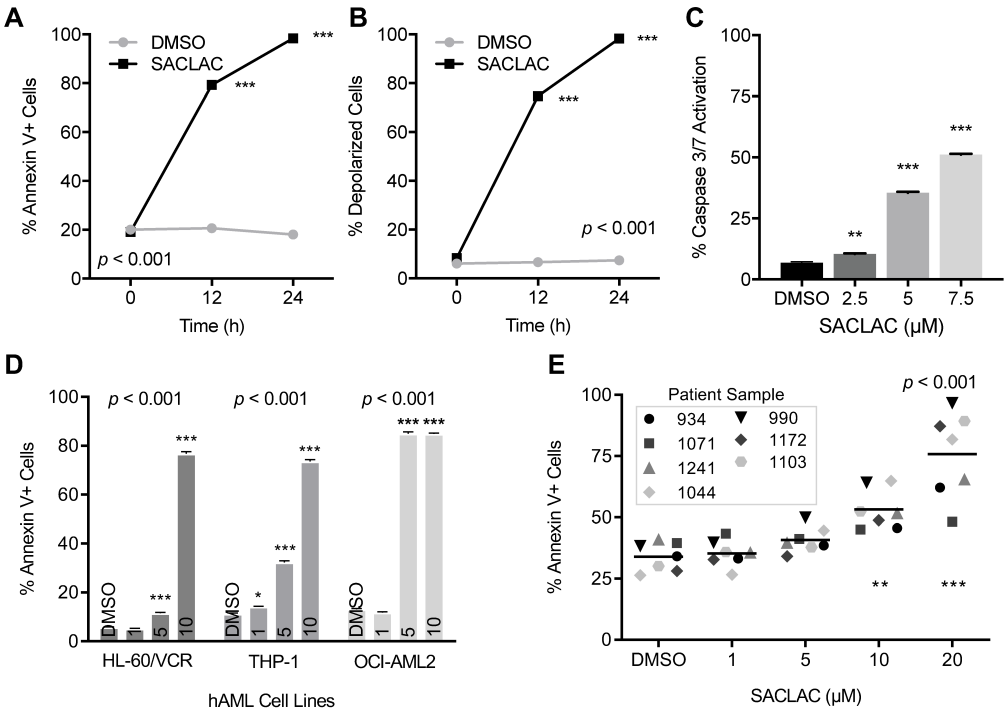

Author Manuscript Published OnlineFirst on November 19, 2019; DOI: 10.1158/1541-7786.MCR-19-0619
Author manuscripts have been peer reviewed and accepted for publication but have not yet been edited.

Figure 4. SACLAC reduces expression of SF3B1 and increases pro-apoptotic Mcl-1S.

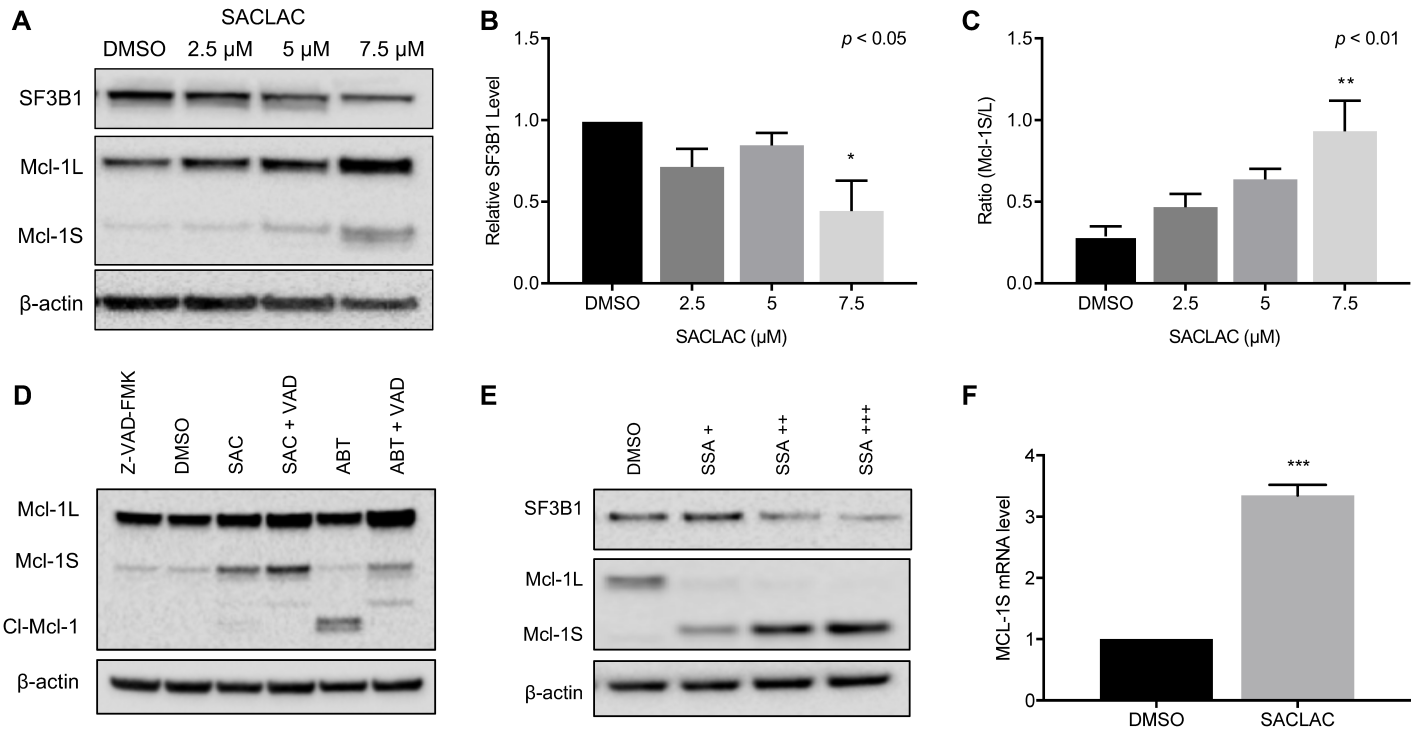

Figure 5. C16 ceramide treatment and AC knockdown reduce SF3B1 and increase Mcl-1S to L ratio.

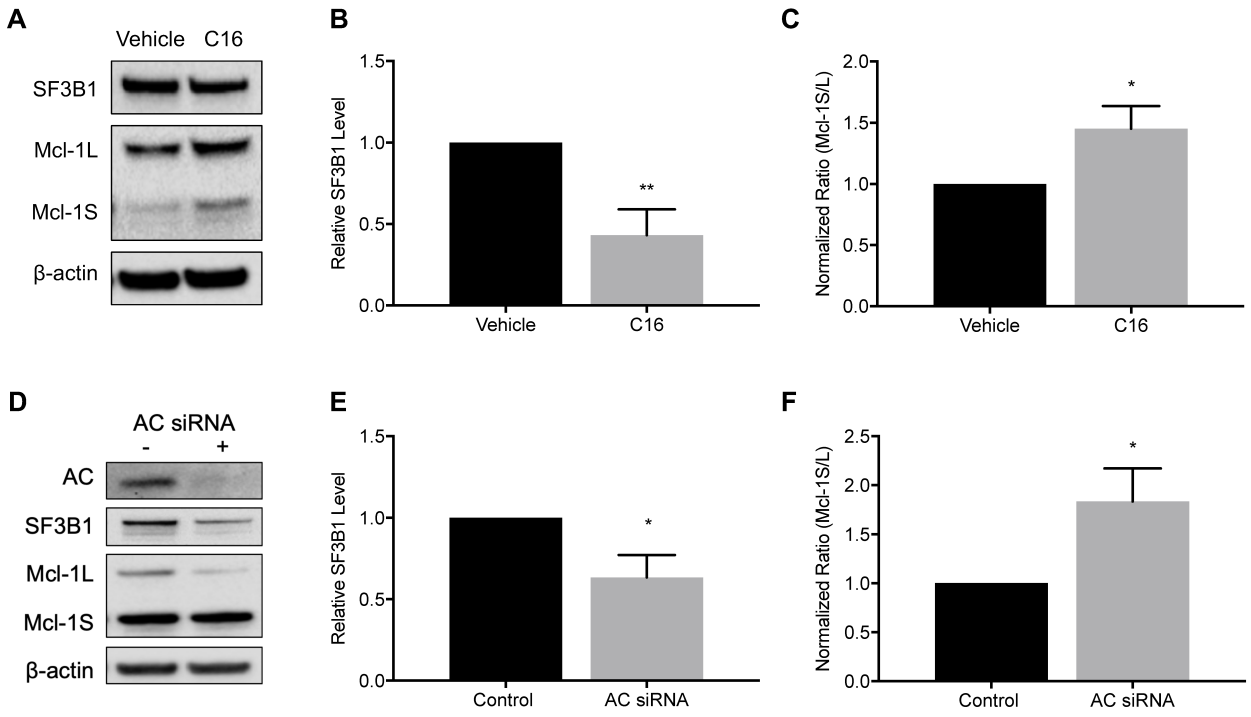

Author Manuscript Published OnlineFirst on November 19, 2019; DOI: 10.1158/1541-7786.MCR-19-0619
Author manuscripts have been peer reviewed and accepted for publication but have not yet been edited.

Figure 6. Altering expression of Mcl-1 and SF3B1 attenuates induction of apoptosis in SACLAC-treated cells.

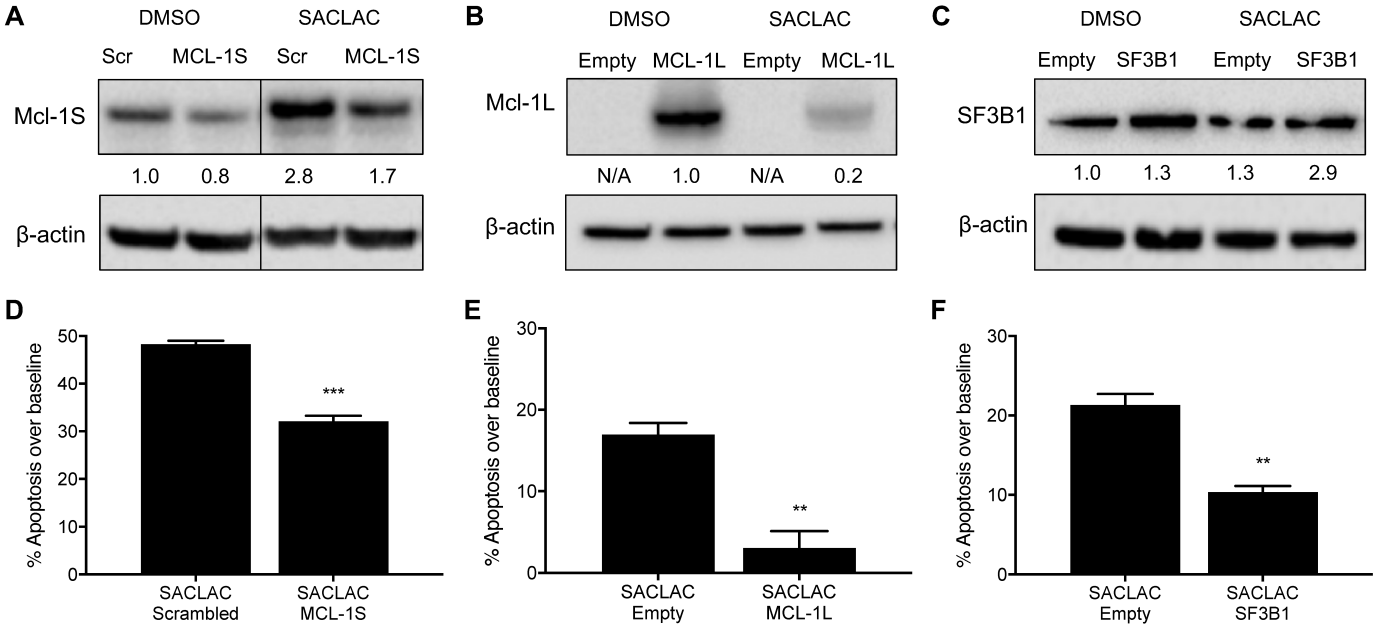

Author Manuscript Published OnlineFirst on November 19, 2019; DOI: 10.1158/1541-7786.MCR-19-0619
Author manuscripts have been peer reviewed and accepted for publication but have not yet been edited.

Figure 7. SACLAC reduces leukemic burden in NSG mouse models of AML.

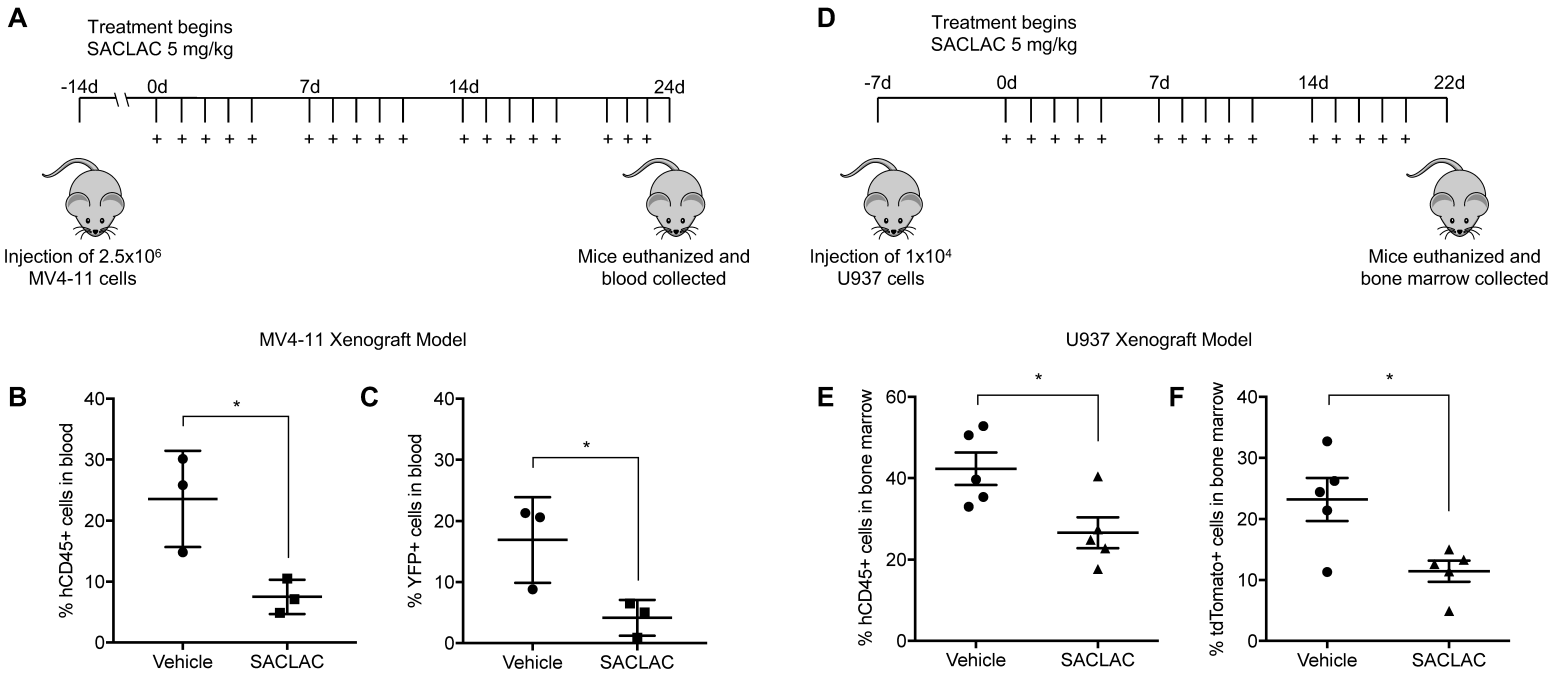

AACR American Association for Cancer Research

Molecular Cancer Research

Ceramide analog SACLAC modulates sphingolipid levels and Mcl-1 splicing to induce apoptosis in acute myeloid leukemia

Jennifer M Pearson, Su-Fern Tan, Arati Sharma, et al.

Mol Cancer Res Published OnlineFirst November 19, 2019.

SUPPLEMENTARY APPENDIX

Ceramide analog SACLAC modulates sphingolipid levels and Mcl-1 splicing to induce apoptosis in acute myeloid leukemia

Jennifer M. Pearson[1], Su-Fern Tan[2], Arati Sharma[3], Charyguly Annageldiyev[3], Todd E. Fox[4], Jose Luis Abad[5], Gemma Fabrias[5], Dhimant Desai[6], Shantu Amin[6], Hong-Gang Wang[3,7], Myles C. Cabot[8], David F. Claxton[3], Mark Kester[4,9], David J. Feith[2,9] and Thomas P. Loughran, Jr[2,9]*

[1] Department of Biochemistry and Molecular Genetics, University of Virginia, Charlottesville, VA, USA
[2] Department of Medicine, Division of Hematology & Oncology, University of Virginia, Charlottesville, VA, USA
[3] Penn State Cancer Institute, Hershey, PA, USA
[4] Department of Pharmacology, University of Virginia, Charlottesville, VA, USA
[5] Department of Biological Chemistry, Institute for Advanced Chemistry of Catalonia, Spanish National Research Council (IQAC-CSIC), Barcelona, Spain
[6] Department of Pharmacology, Penn State College of Medicine, Hershey, PA, USA
[7] Department of Pediatrics, Penn State College of Medicine, Hershey, PA, USA
[8] Department of Biochemistry and Molecular Biology, East Carolina Diabetes and Obesity Institute, Brody School of Medicine, East Carolina University, Greenville, NC, USA
[9] University of Virginia Cancer Center, Charlottesville, VA, USA

*Corresponding Author:
Thomas P. Loughran, Jr.
tl7cs@hscmail.mcc.virginia.edu

CELL LINE RRIDs

CELL LINE	RRID
EOL-1	CVCL_0258
HEL	CVCL_2481
HL-60	CVCL_0002
HL-60/ABTR	N/A
HL-60/VCR	CVCL_0305
Kasumi-1	CVCL_0589
Kasumi-3	CVCL_0612
Kasumi-6	CVCL_0614
KG1	CVCL_0374
KG1/ABTR	N/A
KG1a	CVCL_1824
KG1a/ABTR	N/A
ME-1	CVCL_2110
ML2	CVCL_1418
MM-6	CVCL_1426
MOLM-13	CVCL_2119
MOLM-14	CVCL_7916
MV4-11	CVCL_0064
NB4	CVCL_0005
NOMO1	CVCL_1609
OCI-AML2	CVCL_1619
OCI-AML3	CVCL_1844
OCI-AML4	CVCL_5224
OCI-M2	CVCL_2150
SET2	CVCL_2187
SKM1	CVCL_0098
SNKO1	CVCL_2196
TF-1	CVCL_0559
THP-1	CVCL_0006
U937	CVCL_0007

SUPPLEMENTARY FIGURES

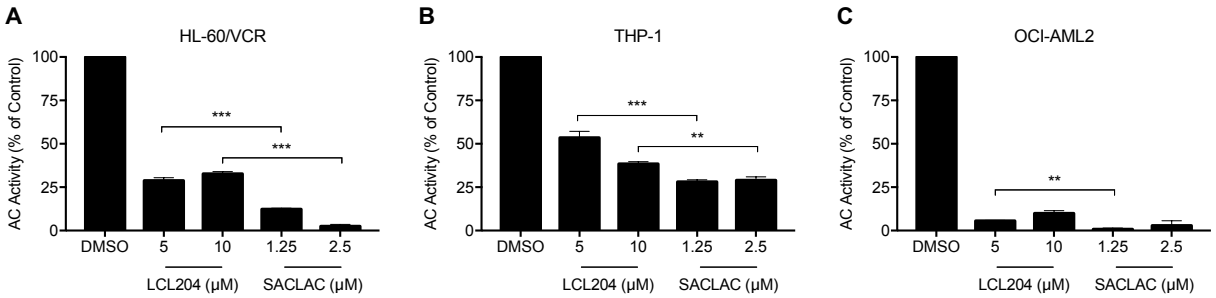

Figure S1. SACLAC reduces AC activity at lower doses than LCL204. A fluorogenic substrate was used to measure AC activity after treatment with DMSO vehicle, LCL204 (5 or 10 μM) or SACLAC (1.25 or 2.5 μM) in **A)** HL-60/VCR, **B)** THP-1 and **C)** OCI-AML2 cell lines. These experiments were repeated twice with equivalent results, and one representative experiment is shown. To demonstrate that SACLAC is more potent than LCL204, comparisons were done on 4X concentrated LCL204 versus 1X SACLAC (5 vs. 1.25 and 10 vs. 2.5 μM) using two-tailed unpaired *t*-test. ** $p < 0.01$, *** $p < 0.001$.

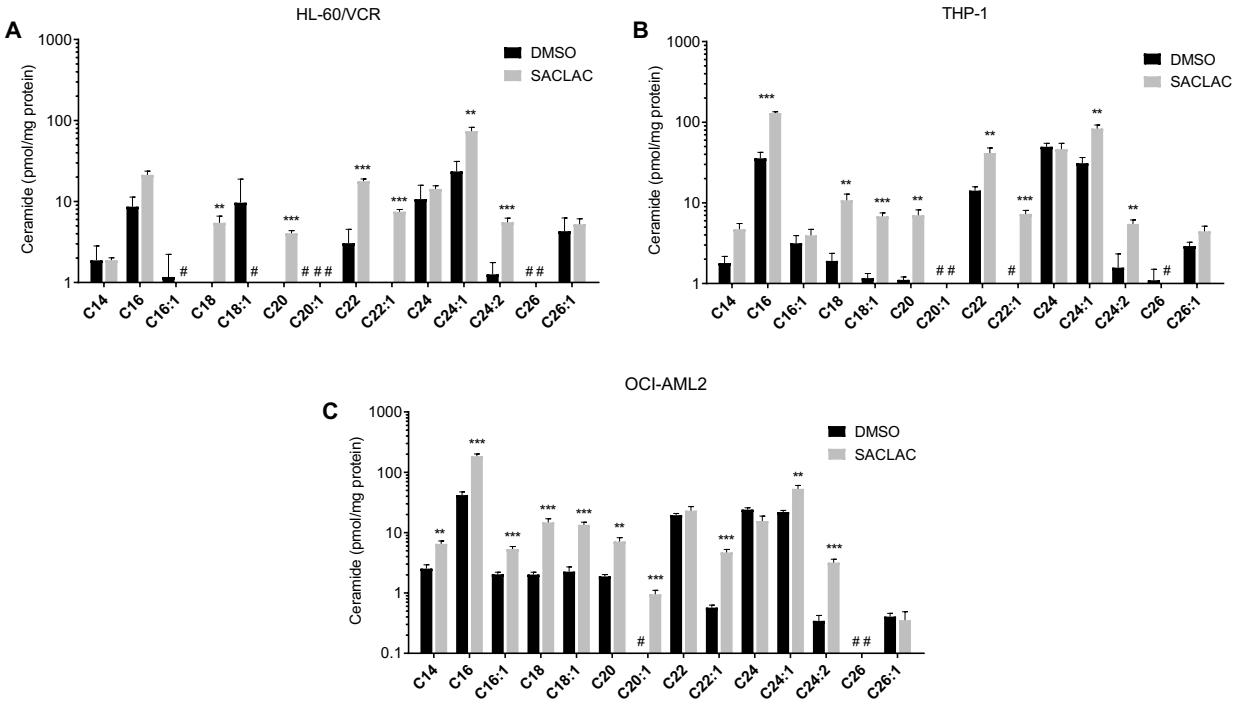

Figure S2. SACLAC treatment increases production of multiple ceramide species in human AML cell lines. Mass spectrometry was used to measure ceramide content after treatment with DMSO vehicle or SACLAC (2.5 μM) for 24 hours in **A)** HL-60/VCR, **B)** THP-1 and **C)** OCI-AML2 cell lines. The y-axis shown is $\log_{10}$ to accommodate all species on an unbroken axis. Each bar represents the mean ± SEM of 5 independent biological replicates from a single experiment. Similar response was observed at other doses (1.25 and 5 μM) of SACLAC. * $p < 0.05$, ** $p < 0.01$, *** $p < 0.001$. # indicates that bar value falls below lower axis limit. Comparison of DMSO versus SACLAC for each ceramide species was evaluated using two-tailed unpaired *t*-test. *p*-values were corrected for multiple testing using the Holm-Sidak method.

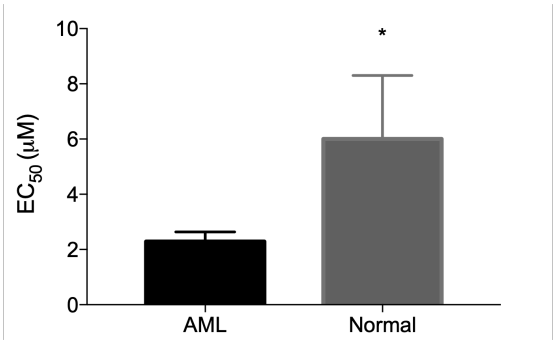

Figure S3. SACLAC is more toxic to AML cells than normal cells. Pooled EC_{50} values are depicted for 29 AML cell lines (AML, n=29) and four normal CD34+ samples and six normal PBMC samples (Normal, n=10). Comparison of AML cell lines versus normal cells was done using two-tailed unpaired *t*-test. * $p < 0.05$.

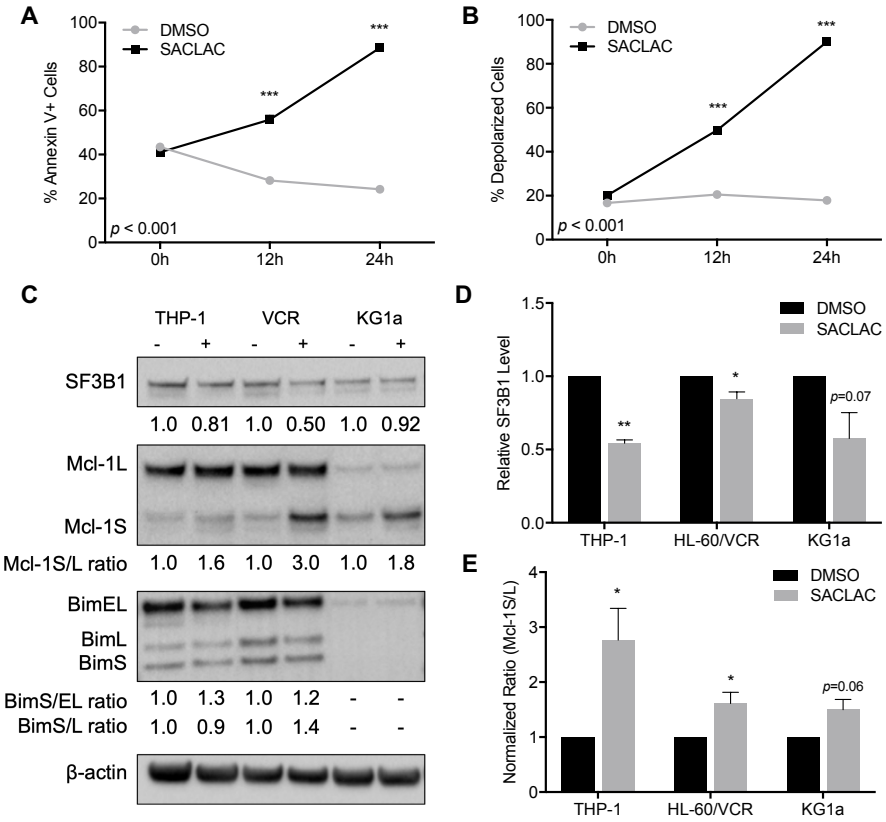

Figure S4. SACLAC mechanism of action is consistent in multiple human AML cell lines. THP-1 cells were treated with DMSO or SACLAC (10 μM) for 0 to 24 hours and evaluated for **A)** apoptosis and **B)** mitochondrial membrane depolarization. Data presented is from one of two independent experiments with equivalent results. **C)** THP-1, HL-60/VCR, and KG1a cells were treated with DMSO (-) or 20 μM SACLAC (+) for 48 hours and assayed for protein levels via western blotting. A representative blot is shown with fold change relative to DMSO and normalized to β-actin (SF3B1) or the specified isoform ratios listed below the blots (Mcl-1 and Bim). **D)** SF3B1 level and **E)** Mcl-1S/L ratio from three independent experiments completed as in panel C were quantified by normalizing to β-actin loading and compared to DMSO control. * $p < 0.05$, ** $p < 0.01$, *** $p < 0.001$. For graphs A and B, the global *p*-value (ANOVA) is presented along with asterisks denoting significance of each time point of SACLAC treatment relative to time 0 using Dunnett's test. Values in panel C show quantification of Mcl-1L (upper) and Mcl-1S (lower) relative to DMSO (set to 1). For graphs D and E, SACLAC treatment was compared to DMSO for each cell line and analyzed using two-tailed unpaired *t*-test.

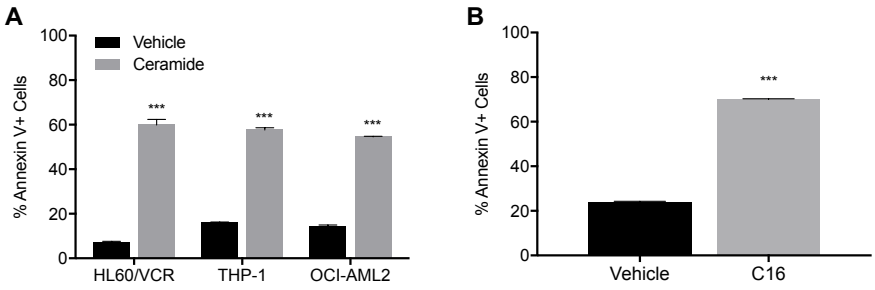

Figure S5. Exogenous ceramides induce apoptosis in human AML cell lines. A) HL-60/VCR, THP-1 and OCI-AML2 human AML cell lines were treated with long-chain ceramide mixture (100 µg/ml) and assayed for apoptosis at 48 hours. **B)** OCI-AML2 cells were treated with DMSO or C16 ceramide (20 µM) for 48 hours and assayed for apoptosis. Comparison of vehicle versus ceramide was done using two-tailed unpaired *t*-test. *** $p < 0.001$. Bars represent mean ± SEM of three independent experiments.

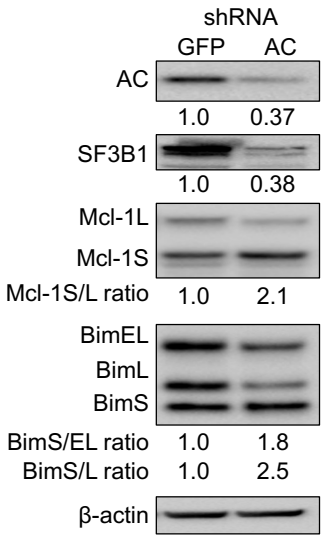

Figure S6. AC knockdown alters splicing of Mcl-1 and Bim in HL-60/VCR cells via regulation of SF3B1. HL-60/VCR cells were transduced with lentivirus containing shRNA to target AC or GFP control for 96 hours. Western blotting of protein lysates was used to confirm AC knockdown efficiency and to determine alterations in the splicing protein, SF3B1, and its targets Mcl-1 and Bim. Band intensity in GFP shRNA samples was set to 1 for normalization. AC and SF3B1 levels were also normalized to β-actin loading control, and the relative values are listed below the blot. For Mcl-1 and Bim, the ratio of short to long isoform(s) is shown.

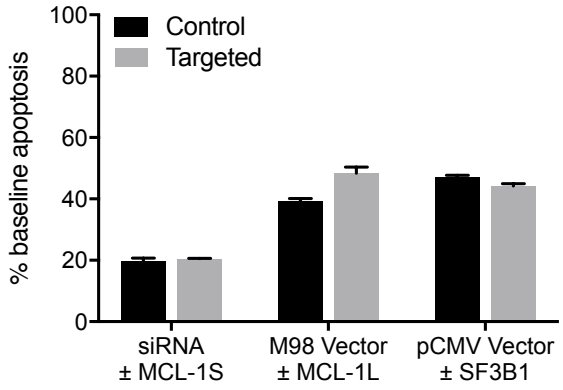

Figure S7. Baseline apoptosis varies based on type of electroporated content. Cells were electroporated with control (non-targeting siRNA or empty vector) or targeted agent (targeting siRNA or targeting cDNA expression vector) and then treated with DMSO vehicle control to determine baseline toxicity with each manipulation.

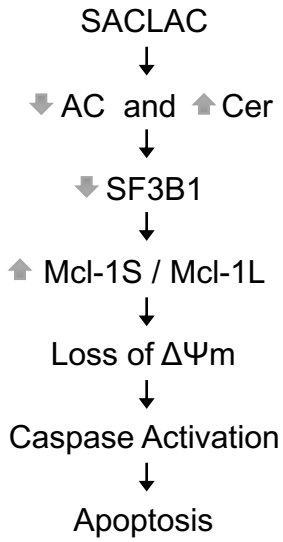

Figure S8. Proposed model of SACLAC mechanism of action. SACLAC treatment inhibits AC which leads to increased ceramide and decreased SF3B1. As ceramide accumulates, alternative splicing of Mcl-1 results in Mcl-1S accumulation that facilitates mitochondrial membrane depolarization. With loss of mitochondrial membrane potential ($\Delta\Psi m$), pro-apoptotic signals are released to activate caspases and induce apoptosis.

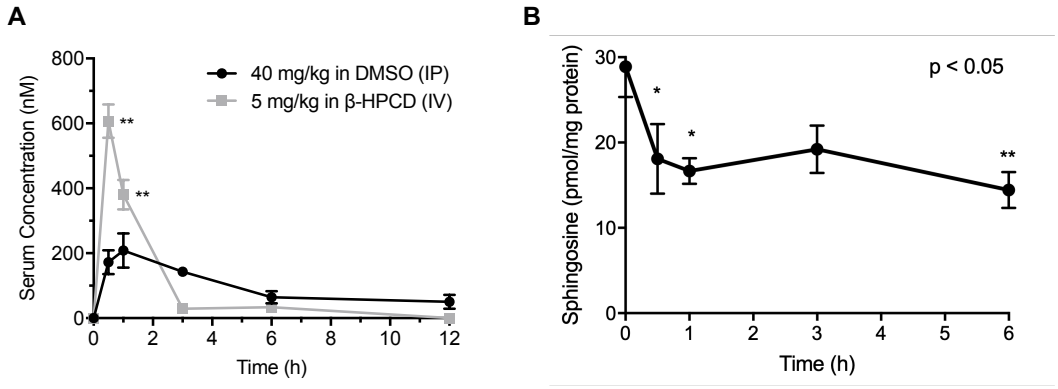

Figure S9. IV administration of SACLAC improves delivery and lipids are shifted in mice. SACLAC was administered to Swiss Webster mice intraperitoneally in DMSO (40 mg/kg) or intravenously in β-HPCD (5 mg/kg). Animals were killed at the indicated time points and concentration of **A)** SACLAC in the blood or **B)** sphingosine in the liver was measured by mass spectrometry. Values represent mean ± SEM from 3 mice per time point. Comparison between DMSO and β-HPCD concentration was evaluated using two-tailed unpaired *t*-test. Change in sphingosine was evaluated using ANOVA followed by Dunnett's test comparing each time point to 0 hours. * $p < 0.05$; ** $p < 0.01$.